ACS Chemical Neuroscience



pubs.acs.org/chemneuro
Research Article

# Monoamine Oxidase Inhibitors Present in Tobacco Modulate Dopamine Balance Via the Dopamine Transporter

Gabriella Saro,* Stephanie Johne, Diogo A.R.S. Latino, Fabian Moine, Marco van der Toorn, Carole Mathis, and Emilija Veljkovic

Cite This: ACS Chem. Neurosci. 2025, 16, 1117−1131
Read Online



**ABSTRACT:** It has been reported that nicotine affects brain dopamine homeostasis. By binding to nicotinic acetylcholine receptors, including those expressed by dopaminergic neurons of the ventral tegmental area, nicotine stimulates dopamine release and signaling. Dopamine is taken up from the synaptic cleft by the dopamine transporter (DAT) into presynaptic neurons, where it is degraded by monoamine oxidase (MAO). Besides nicotine, other tobacco compounds play a role in dopamine modulation. To better understand the biological effects of nicotine and other tobacco compounds on dopamine regulation, we selected a group of tobacco compounds based on their potential affinity to bind human MAO-A and MAO-B enzymes using an *in silico* approach. Subsequently, we tested the putative compounds in an enzymatic assay to verify their ability to inhibit human MAO-A or MAO-B. The positive hits were harman, norharman, harmaline, and 1-ethyl-*β*-carboline. While harman and norharman have been extensively studied, both harmaline and 1-ethyl-*β*-carboline have not been described in the context of tobacco and MAO inhibition before. We investigated DAT activity in an overexpressing cell line and dopamine release and uptake in rat striatal synaptosomes. We clearly demonstrate that tested MAO-A inhibitors (MAO-AIs) significantly attenuated human DAT activity and consequent dopamine uptake, establishing a functional connection between MAOIs and dopamine uptake via DAT. Interestingly, the tested MAO-AIs elicited pronounced dopamine release in crude synaptosomal preparations. In summary, this *in vitro* study demonstrates that tested MAO-AIs found in cigarette smoke not only reduce MAO activity but also strongly impact dopamine homeostatic mechanisms via DAT. Further *in vivo* investigations would advance our understanding of the underlying mechanisms of dopamine regulation and homeostasis.

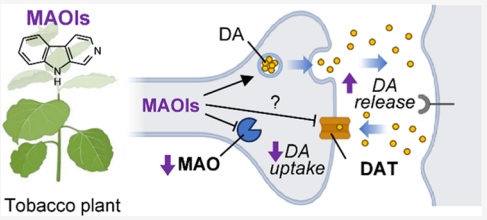


**KEYWORDS:** *monoamine oxidase inhibitors, nicotine, dopamine, dopamine transporter, β, carbolines, neurotransmission*

## INTRODUCTION

The reinforcing properties of cigarette smoke (CS) are largely driven by nicotine effects, which are the most studied. To date, the molecular mechanisms underlying nicotine reinforcement remain somewhat unknown.[1] Upon smoking, nicotine enters the bloodstream of the airways via smoke particles, crosses the blood−brain barrier (BBB), and reaches critical brain regions such as the mesolimbic area, striatum, and frontal cortex. The mesolimbic reward pathway mediates the perception of environmental cues that are sensed as pleasurable.[2,3] The reward pathway includes the ventral tegmental area (VTA) and nucleus accumbens (NAc). These two areas are connected by dopamine projections from the VTA, which express nicotinic acetylcholine receptors (nAChRs), a heterogeneous family of pentameric, ligand-gated, cation-selective channels responsive to both acetylcholine and nicotine.[4] Activation of nAChRs triggers ion influx ($Ca^{2+}$, $Na^{+}$) into the VTA dopaminergic neurons, leading to dopamine release in the NAc. The released dopamine elicits a reward response via binding and activation of dopaminergic receptors on postsynaptic neurons. To regulate central neurotransmission, dopaminergic signals diminish upon dopamine reuptake from the synaptic cleft through the dopamine transporter (DAT) and degradation by the enzyme monoamine oxidase (MAO). The DAT is a $Na^{+}$/$Cl^{-}$-dependent transporter that can transport molecules against their gradient.[5] DAT localizes in dopaminergic neurons that are part of mesolimbic, mesocortical, and mesostriatal brain pathways.[5] In *DAT* knockout mice, intracellular dopamine stores are depleted, despite the higher rate of dopamine synthesis,[6] suggesting that DAT-mediated reuptake is crucial for a stable intracellular dopamine pool. MAOs are flavoenzymes anchoring to the outer mitochondrial membrane and exist as two isoenzymes: MAO-A and MAO-B. The type A isoform has been localized to several neuronal cell types in primates and rodents, including noradrenergic neurons of the locus coeruleus, dopaminergic neurons of the substantia nigra pars compacta and striatal medium spiny neurons.[7] However,

Received: November 22, 2024
Revised: February 19, 2025
Accepted: February 21, 2025
Published: March 4, 2025

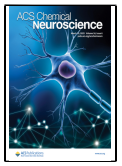





https://doi.org/10.1021/acschemneuro.4c00789
ACS Chem. Neurosci. 2025, 16, 1117−1131

Table 1. List of Tested Candidate MAOIs[a]

| N° | compound name | CAS | binding affinity docking MAO-A 2Z5X [kcal/mol] | binding affinity docking MAO-B 2 V5Z [kcal/mol] | BIOVIA log of brain/blood partition coefficient log (BBB) | AdmetSAR BBB probability of permeation | BIOVIA BBB penetration level |
|---|---|---|---|---|---|---|---|
| 1 | 5-cyanonicotine (*) | 42459−12−1 | −6.49 | −6.55 | −0.406 | 0.9972 | medium |
| 2 | harman (*) | 486−84−0 | −6.35 | −5.81 | 0.188 | 1 | high |
| 3 | 9H-pyrido[3,4-*b*] indole, 1-ethyl (*) | 20127−61−1 | −6.74 | −6.63 | 0.394 | 1 | high |
| 4 | 2-methyl-3-phenylpyrazine (*) | 29444−53−9 | −6.01 | −5.97 | 0.033 | 0.9941 | high |
| 5 | nicotelline (*) | 494−04−2 | −7.35 | −7.16 | −0.119 | 0.9955 | medium |
| 6 | harmaline (*) | 304−21−2 | −7.22 | −7.13 | 0.052 | 0.9909 | high |
| 7 | norharman (*) | 244−63−3 | −5.85 | −5.76 | 0.101 | 1 | high |
| 8 | myosmine (*) | 532−12−7 | −6.23 | −5.73 | −0.222 | 0.9974 | medium |
| 9 | 2,3′-bipyridyl (*) | 581−50−0 | −5.85 | −5.77 | −0.054 | 0.9955 | medium |
| 10 | N-nitrosoanatabine (*) | 887407−16−1 | −6.61 | −6.84 | −0.147 | 0.9819 | medium |
| 11 | 2,2′-bipyridyl (*) | 366−18−7 | −5.87 | −5.74 | 0.078 | 0.9968 | high |
| 12 | anatabine (*) | 581−49−7 | −6.23 | −5.83 | −0.271 | 0.9965 | medium |
| 13 | 5-methoxy-3-(2-pyridinylmethyl)-1H-indole | 101832−06−8 | −7.71 | −7.49 | 0.164 | 0.9953 | high |
| 14 | 2,7,12-cyclotetra dec atrien-1-ol,1,7-dimethyl-11methylene-4-(1-methylethyl)- | 60026−11−1 | −5.29 | −8.18 | 1.253 | 0.9612 | very high |
| 15 | tetrahydro-1H-betacarbolin-1-yl acetone | 69225−88−3 | −7.44 | −7.66 | −0.319 | 0.994 | medium |
| 16 | *β*-nicotyrine | 487−19−4 | −5.89 | −5.74 | 0.136 | 0.9948 | high |
| 17 | pyridine, 3-[1-(5-propyl-2-furanyl)-1Hpyrrol-2-yl] | 78210−89−6 | −7.59 | −8.02 | 0.578 | 0.9896 | high |
| 18 | N-cyclohexyl-nicotinamide | 10354−56−0 | −7.48 | −7.4 | −0.269 | 0.9955 | medium |
| 19 | 1-[4-amino-2-methyl-5-(2-methylphenyl)-1H-pyrrol-3-yl] ethanone | 56463−76−4 | −6.00 | −7.67 | −0.357 | 0.9696 | medium |

[a]Compounds marked with an asterisk (*) were tested *in vitro*. Abbreviations: Admet: absorption, distribution, metabolism, excretion, and toxicity; BBB: blood−brain barrier; CAS: Chemical Abstracts Service; MAO: monoamine oxidase.

the B isoform is found in glia and astrocytes.[8] Interestingly, specific compounds with the ability to inhibit MAO enzymes have been identified in CS.[9] Since MAO inhibitors (MAOIs) hinder dopamine degradation, a potentiated dopaminergic system is seen in association with smoking.[10]

While nicotine itself is a relatively weak reinforcer of the brain monoamine system *in vivo*,[11] recent investigations suggest that non-nicotinic components of CS[12,13] may contribute to the psychoactive effects of CS, possibly via an additive or synergistic action on nicotine.[14−16] Among the non-nicotinic components in CS, molecules belonging to the chemical class of *β*-carbolines showed MAO inhibitory activity and are therefore considered as MAOIs.[17] MAOIs have been extensively studied and are likely to play a significant role in this phenomenon. After quitting smoking, people experience a withdrawal effect due to increased dopamine degradation by MAO-A. A positron emission tomography study showed that smokers have reduced MAO-A activity in the brain compared to nonsmokers and that this reduction was 28% on average in different brain regions.[18] Studies in rats injected with tobacco-derived MAOIs demonstrated increased self-administration of low nicotine doses (10−15 *μ*g/kg/infusion) and decreased self-administration of high nicotine doses (60−90 *μ*g/kg/infusion), suggesting that MAO inhibition enhances sensitivity to nicotine's rewarding effects.[16,19,20]

Further evidence suggests that cigarette smoke extract (CSE) reduced the effect of MAO-A/B activities *in vitro*, whereas nicotine alone did not.[21] Another study showed that MAO-A was irreversibly inhibited *in vitro* in rat brain mitochondrial homogenates incubated with CSE, which was not the case *in vivo* probably due to the low concentration of MAOIs contained in the CSE or brain permeability.[21] In another self-administration study in rats, either nicotine, norharman, or a combination of both were available. Norharman reinforced the self-administration behavior but, in combination with nicotine, it activated different neuronal patterns than those activated by either nicotine or norharman alone,[22] further confirming the important role of MAOIs in reward processing. Additionally, previous studies have shown that the MAO-AI harmine potentiates electrically evoked dopamine efflux in the shell of the NAc[23] as well as in brain slices, similar to harmaline.[24] Numerous MAOIs belonging to the chemical family of *β*-carbolines were found to reduce dopamine reuptake in rat striatal synaptosomes.[25] Of note, the potentiation of the reward pathway requires the regulation of dopamine neurotransmission by DAT and MAO, which are crucial targets mediating this mechanism. Nevertheless, the current understanding is lacking evidence on the underlying pharmacological mechanism of MAOIs in the monoaminergic system in the context of reward.

The present study sought to elucidate how individual tobacco-derived molecules—other than nicotine—act on reward system regulation by examining its fundamental elements: dopamine release, dopamine uptake, DAT activity,


https://doi.org/10.1021/acschemneuro.4c00789
ACS Chem. Neurosci. 2025, 16, 1117−1131

and MAO activity. By engaging a computational chemistry approach and pharmacophore analysis, we identified potential MAOI candidates that were confirmed using *in vitro* enzymatic MAO assays. Among these compounds, harman and norharman have been extensively studied and provide solid benchmarks for our approach. Additionally, we found the less well-studied MAO-AIs harmaline and 1-ethyl-$\beta$-carboline, the latter newly identified as an MAO-AI in association with CS. With subsequent investigation in cellular and *ex vivo* models of dopamine release and uptake, we identified the tobacco-derived MAOIs that might reinforce dopaminergic balance with potential effects on the brain's reward system.

## RESULTS AND DISCUSSION

**_In Silico_ Identification of Potential MAO-A and MAO-B Inhibitors Present in Tobacco Smoke.** To identify novel MAOIs in data sets of candidate compounds from tobacco, we conducted a computational chemical analysis followed by *in vitro* screening for MAO activity. The computational process followed three major steps: (i) retrieving data sets of known MAOIs from the literature and data sets of compounds identified and quantified in tobacco smoke, (ii) encoding the data sets using pharmacophore descriptor approaches, and (iii) calculating the pharmacophore similarities between known MAOIs and tobacco compounds from the data sets. This approach allowed us to identify the tobacco compounds that were most similar to known MAOIs. Since the resulting number of potential MAOIs was considerably high for experimental screening, additional parameters were used as selection criteria: (i) the compound should be present in the fully characterized tobacco molecules list published by Bentley et al.[26] with the highest identification confidence (confirmation using reference standard). (ii) The compound should be predicted to cross the BBB by *in silico* estimations. (iii) The compound needs to be commercially available.

Using an *in silico* pharmacophore approach, 19 compounds present in Bentley et al.[26] were identified as potential MAO-A and MAO-B inhibitors. The compound database used does not present a complete list of compounds and was not intended to be used as a standard list of compounds in tobacco product emissions. The list is a result of a comprehensive identification and quantification of compounds in tobacco product emission with a threshold above 100 ng/item. The full list of candidate compounds and their affinity for human MAO-A and MAO-B are displayed in Table 1. The binding affinity docking score was observed in the range of −5.29 to −7.71 (kcal/mol) for MAO-A 2Z5X and in the range of −5.73 to 8.18 (kcal/mol) for MAO-B 2 V5Z. Among the 19 compounds, 12 were confirmed using authentic analytical reference materials: 5-cyanonicotine; harman; 9H-pyrido[3,4-*b*] indole, 1-ethyl; 2-methyl-3-phenylpyrazine; nicotelline; harmaline; norharman; myosmine; 2,3′-bipyridyl, N-nitrosoanatabine; 2,2′-bipyridyl; and anatabine (Table 1, compounds marked by an asterisk). The remaining 7 compounds were listed as follows: 5-methoxy-3-(2-pyridinylmethyl)-1H-indole; 2,7,12-cyclotetradecatrien-1-ol,1,7-dimethyl-11methylene-4-(1-methylethyl); tetrahydro-1H-betacarbolin-1-yl acetone; $\beta$-nicotyrine, pyridine, 3-[1-(5-propyl-2-furanyl)-1Hpyrrol-2-yl]; N-cyclohexyl nicotinamide; and 1-[4-amino-2-methyl-5-(2-methylphenyl)-1H-pyrrol-3-yl] ethenone. These 7 compounds were not formally identified, as they would have needed to be confirmed against their analytical standard.

Among the 19 compounds, all were predicted to have the potential to cross the BBB using the two approaches (admetSAR and the BIOVIA ADMET BBB Model [BIOVIA, San Diego, CA]). The admetSAR tool predicted all compounds with a high probability of permeation with values between 0.96 and 1 (indicating a maximal probability of permeation). The BIOVIA BBB model estimated that all compounds were in the "medium" to "very high" BBB penetration level, in line with the admetSAR model. The BBB permeability parameters of the candidate compounds are displayed in Table 1.

**Confirming the MAO Inhibitory Activity of Compounds Identified _In Silico_ using an _In Vitro_ Enzymatic Assay.** The 12 compounds identified as potential MAOIs by our *in silico* approaches were assessed *in vitro* for their inhibitory properties against both human MAO-A and MAO-B enzymes using the MAO-Glo enzymatic assay. The $IC_{50}$ values are summarized in Table 2 for both MAO-A and MAO-B.

**Table 2. Determination of Half-Maximal Inhibitory Concentration ($IC_{50}$) of MAO Inhibitors Identified In Silico[a]**

| compound name | MAO-A inhibition mean $IC_{50}$ value [$\mu$M] | MAO-B inhibition mean $IC_{50}$ value [$\mu$M] |
|---|---|---|
| harmaline | 0.02 | |
| harman | 0.06 | |
| M30 hydrochloride (MAO-A control) | 0.90 | |
| 1-ethyl-$\beta$-carboline | 1.69 | |
| norharman | 1.70 | 7.30 |
| pargyline (MAO-B control) | | 3.78 |

[a]Abbreviations: $IC_{50}$: half-maximal inhibitory concentration; MAO: monoamine oxidase.

Control compounds M30 hydrochloride (Figure S1A) for MAO-A inhibition [$IC_{50}$: 0.9 $\mu$M] and pargyline (Figure S1B) for MAO-B inhibition [$IC_{50}$: 3.78 $\mu$M] were tested as positive controls for the assay. Among all the candidate compounds tested (data not shown), four compounds successfully inhibited the human MAO-A enzyme at the following $IC_{50}$ values: harman (Figure S1C), norharman (Figure S1F,G), harmaline (Figure S1E), and 9H-pyrido[3,4-*b*] indole, 1-ethyl (referred to as 1-ethyl-$\beta$-carboline from here on) (Figure S1D). Notably, the in silico approach was able to identify already reported MAOIs from the list of screened tobacco compounds and interestingly the predicted binding affinities of three known MAOIs, harmaline, harman, and norharman, with predicted binding affinities of −7.22, −6.35, and −5.85 kcal/mol, were fairly ranked when compared with the experimental $IC_{50}$s of 0.02, 0.06, and 1.70 $\mu$M, respectively, measured *in vitro* in the MAO activity assay (Table 2). The three identified compounds harman, norharman, and harmaline are known to be reversible MAO-A and MAO-B (for norharman) inhibitors.[9] The compound 1-ethyl-$\beta$-carboline has not been confirmed as a reversible or irreversible MAOI. On the other hand, the compounds 5-cyanonicotine, 2-methyl-3-phenylpyrazine, nicotelline, myosmine, 2,3′-bipyridyl, N-nitrosoanatabine, 2,2′-bipyridyl, and anatabine did not show any inhibitory properties with the MAO-A enzyme using the enzymatic assay. Furthermore, norharman [$IC_{50}$: 7.30 $\mu$M], successfully inhibited human MAO-B, (Figure S1G) while the 11 other candidate compounds identified *in silico* did not


https://doi.org/10.1021/acschemneuro.4c00789
ACS Chem. Neurosci. 2025, 16, 1117−1131

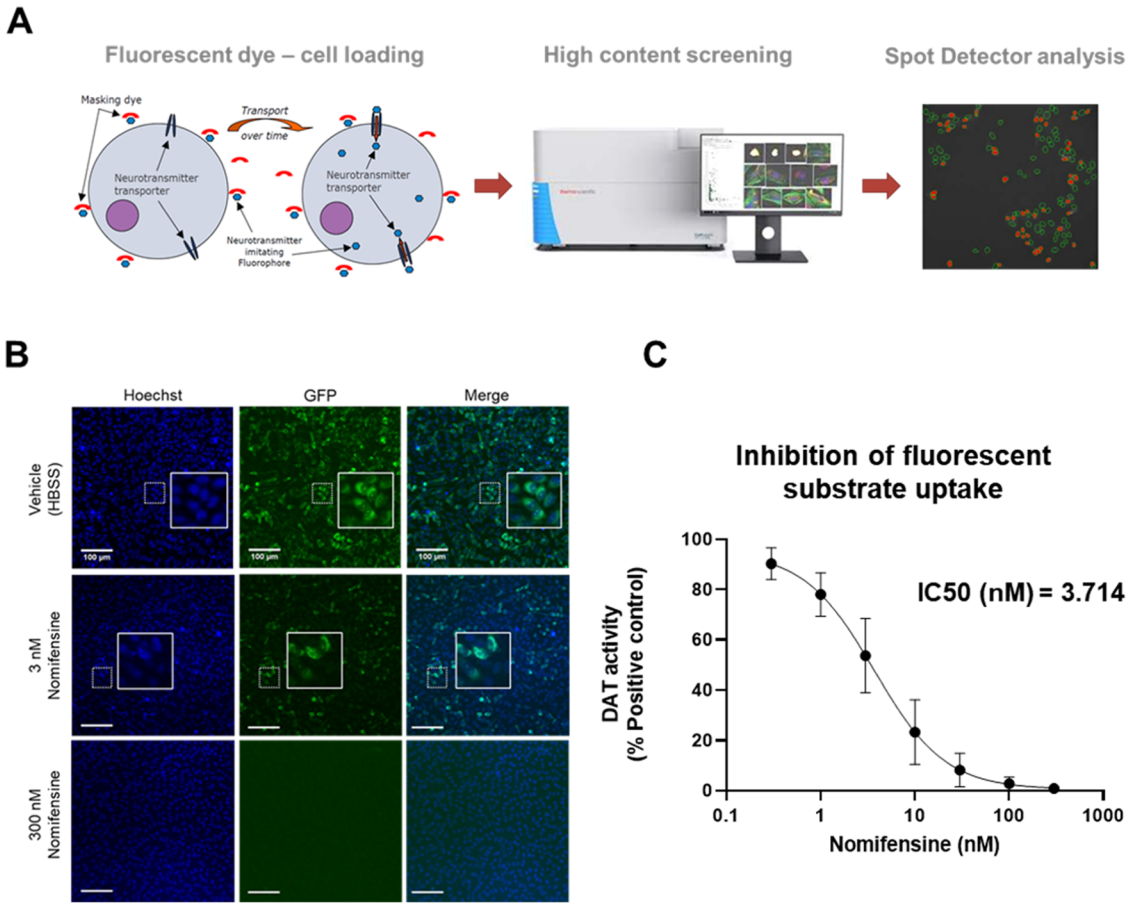


**Figure 1.** *In vitro* DAT activity assay and specific inhibition by nomifensine. (A) DAT activity assay workflow showing cell loading with fluorescent dye, high-content screening by Thermo CellInsight CX7, and built-in analysis by SpotDetector. (B) High-content screening images showing nuclear staining (Hoechst), uptaken fluorescent dye (GFP), and merge in hDAT-CHO cells in the presence of vehicle, 3 and 300 nM nomifensine. Scale bar = 100 $\mu$m. (C) GFP fluorescence was quantified and plotted in a dose−response curve to show the inhibitory effect of nomifensine on DAT. Data are presented as mean ± standard deviation, $n \geq 3$.

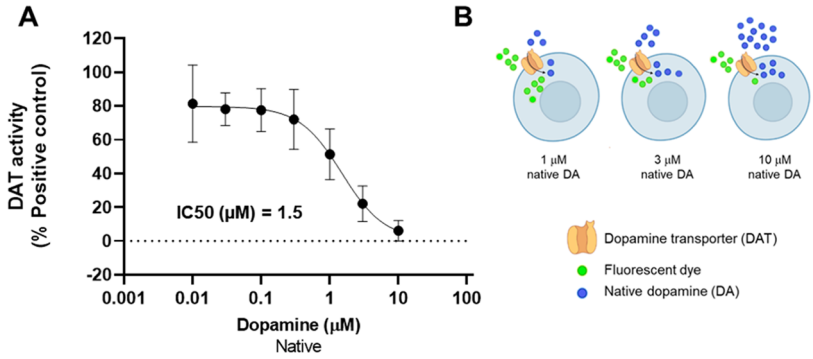


**Figure 2.** Native dopamine competes with the fluorescent dye in DAT-mediated transport. (A) Progressive reduction of fluorescent dye uptake with increasing native dopamine concentrations. Data are presented as mean ± standard deviation, $n \geq 3$. (B) Schematic illustration of reduced fluorescent dye uptake in the presence of increasing native dopamine concentrations (created with BioRender.com).

display any inhibitory properties with MAO-B. Notably, 1-ethyl-$\beta$-carboline was first and only reported by Ho et al. in 1968,[27] and to the best of our knowledge, there was no available information on its MAO docking before our study. Figure S2 displays the docking pose of 1-ethyl-$\beta$-carboline in the orthosteric binding site of the MAO-A crystal structure and compares it with a cocrystallized harmine binding pose. Our compound presents a similar binding pose relative to harmine where the strongest interaction is with a molecule of water bridging the ligand with Ile207 residue, which is also the strongest interaction observed in the cocrystallized harmine with the enzyme.

***In Vitro* DAT Activity Assay Allows Potency and Dose-Range Finding of Selected MAOIs.** The effects of the selected MAOIs directly on the human DAT (hDAT) were further investigated, as it is a crucial element for dopamine uptake and dopaminergic signaling termination. To do so, an assay using a recombinant Chinese Hamster Ovary (CHO)


https://doi.org/10.1021/acschemneuro.4c00789
ACS Chem. Neurosci. 2025, 16, 1117−1131

cell line expressing hDAT was developed as described in the Methods. We detected the DAT-mediated basal uptake of a fluorescent dye mimicking monoamine neurotransmitter by high-content screening (HCS) (Figure 1A). We could verify that the uptake was DAT specific as CHO cells lacking DAT (used as a negative control) failed to take up the dye, as expected (Figure S3A and B). Subsequently, hDAT-CHO cells were pretreated with the specific DAT blocker nomifensine, the fluorescent dye was added, and the resulting fluorescence was quantified by HCS. Fluorescent microscopy images reflected the dose−response effect of nomifensine on DAT activity, as hDAT-CHO cells present maximal fluorescence in the presence of vehicle, approximately 50% fluorescence at 3 nM nomifensine corresponding to the calculated $IC_{50}$ value, and total signal loss indicating no fluorescent dye uptake at the maximal nomifensine concentration corresponding to 300 nM (Figure 1B). The application of nomifensine reduced the uptake with high potency and an $IC_{50}$ value of 3.714 nM (Figure 1C).

To test whether the neurotransmitter uptake assay was specific for both dopamine and DAT, hDAT-CHO cells were preincubated with nonfluorescent dopamine (referred to as "native" from here on) and a fixed dose of the fluorescent substrate (as reported by the manufacturer, 4 $\mu$M at the final concentration). Increasing doses of native dopamine reduced the uptake of the fluorescent substrate in a dose−response dependent manner, with more pronounced effects at 1, 3, and 10 $\mu$M, which are approximately 1:3, 1:1, and 3:1 ratio to the fluorescent substrate, respectively. The result is a dose−response curve for native dopamine with an $IC_{50}$ value of 1.5 $\mu$M (Figure 2A). The reduced fluorescent signal reflects an increasing native dopamine uptake in contrast to the fluorescent dye substrate and suggests competition between native dopamine and the dye (Figure 2B).

For the DAT assay, nicotine, two known MAO-A and MAO-B inhibitors used as positive controls (clorgyline and pargyline, respectively), and the three tobacco-derived MAOIs identified in the enzymatic assay (harman, norharman, and 1-ethyl-$\beta$-carboline) were tested individually in a dose−response mode. Harmaline could not be tested in this assay because its autofluorescence caused crosstalk with the fluorescent dye, even at nanomolar concentrations (data not shown). The $IC_{50}$ values are summarized in Table 3. Nicotine did not induce an optimal dose−response relationship for DAT inhibition (Figure 3A). Pargyline (MAO-B control) application displayed an effect at 30 and 100 $\mu$M only (Figure 3B), whereas clorgyline (MAO-A control) reduced substrate uptake (Figure 3C). All tobacco-derived MAO-AIs dose-dependently reduced the DAT activity. The compound 1-ethyl-$\beta$-carboline was the most potent MAO-AI with an $IC_{50}$ value of 0.66 $\mu$M (Figure 3F), while harman and norharman had $IC_{50}$ values of 1.49 and 3.04 $\mu$M, respectively (Figure 3D,E). This result reveals that the three tested MAO-AIs reduced the DAT activity, whereas the tested MAO-BI pargyline was rather weak.

**Table 3. $IC_{50}$ Values for the *In Vitro* Dopamine Transporter Activity Assay[a]**

| compound name | MAO-A inhibition | MAO-B inhibition | DAT activity $IC_{50}$ [$\mu$M] |
|---|---|---|---|
| nicotine | no | no | unstable |
| 1-ethyl-$\beta$-carboline | yes | no | 0.66 |
| clorgyline (MAO-A control) | yes | no | 0.79 |
| harman | yes | no | 1.49 |
| norharman | yes | yes | 3.04 |
| pargyline (MAO-B control) | no | yes | 20.68 |

[a]Abbreviations: $IC_{50}$: half-maximal inhibition; MAO: monoamine oxidase, DAT: dopamine transporter.

**MAO-A Inhibitors Dose-Dependently Decrease [$^3$H] Dopamine Uptake in Rat Striatal Synaptosomes Contributing to [$^3$H] Dopamine Accumulation.** We next investigated whether selected MAO-AIs might influence dopamine uptake in a more complex system such as rat striatal synaptosomes, which is a widely used model for studying synaptic physiology.[28] Nicotine partially inhibited (45% reduction) [$^3$H] dopamine uptake at 10 $\mu$M (Figure 4A) in synaptosomes, whereas it did not inhibit fluorescent dye uptake in the cellular DAT activity assay. This effect can be explained by the fact that nicotine acts on more targets than DAT alone, such as unknown receptors expressed in synaptosomes that are absent in hDAT-CHO cells. As a specific uptake control, the DAT inhibitor nomifensine was tested, and as expected, it potently inhibited [$^3$H] dopamine uptake with an $IC_{50}$ of 0.044 $\mu$M (Figure 4B) confirming that this mechanism is mediated by DAT, which is in accordance with our data obtained from the DAT *in vitro* assay. The control MAO-BI pargyline reduced [$^3$H] dopamine uptake by 20% at the highest concentration tested (100 $\mu$M), indicating a weak inhibition of [$^3$H] dopamine uptake, consistent with our data from hDAT-CHO cells (Figure 4C). The control MAO-AI clorgyline inhibited [$^3$H] dopamine uptake at 43.3 $\mu$M (Figure 4D). Interestingly, we observed that the MAOIs harman, norharman, harmaline, and 1-ethyl-$\beta$-carboline showed inhibitory effects on [$^3$H] dopamine uptake, with $IC_{50}$ values of 25.4, 29, 22.5, and 18 $\mu$M, respectively (Figure 4E−H and Table 4).

**Selected MAO-A Inhibitors Dampen [$^3$H] Dopamine Entry into Rat Striatal Synaptosomes via the DAT, Confirming Reduced [$^3$H] Dopamine Uptake.** To further confirm our observations from the [$^3$H] dopamine uptake assay, we hypothesized that MAOIs reduce [$^3$H] dopamine loading of synaptosomes via the DAT resulting in reduced [$^3$H] dopamine release. Thus, unloaded synaptosomes were pretreated with MAOIs and then incubated with [$^3$H] dopamine and stimulated with nicotine. After nicotine stimulation, [$^3$H] dopamine release was measured and then synaptosomes were restimulated with 30 mM KCl for maximal depolarization (Figure 5A). Our results show that synaptosomes pretreated with either 10 $\mu$M nomifensine or 100 $\mu$M MAO-AIs did not release any [$^3$H] dopamine upon 1 $\mu$M nicotine stimulation, confirming our hypothesis that these compounds inhibited dopamine uptake via the DAT. Conversely, synaptosomes in the presence of the vehicle and synaptosomes pretreated with the MAO-BI pargyline at 100 $\mu$M, equally released [$^3$H] dopamine upon nicotine stimulation. Untreated synaptosomes (negative control) in the absence of nicotine stimulation showed no [$^3$H] dopamine release. The difference between vehicle, MAO-AIs, and nomifensine was statistically significant (Figure 5B). Final depolarization with 30 mM KCl displayed higher [$^3$H] dopamine release in the untreated, nomifensine-pretreated, vehicle, and pargyline-pretreated synaptosomes (Figure 5C). Clorgyline, harmaline, and 1-ethyl-$\beta$-carboline showed lower [$^3$H] dopamine release compared to the controls due to poor


https://doi.org/10.1021/acschemneuro.4c00789
ACS Chem. Neurosci. 2025, 16, 1117−1131

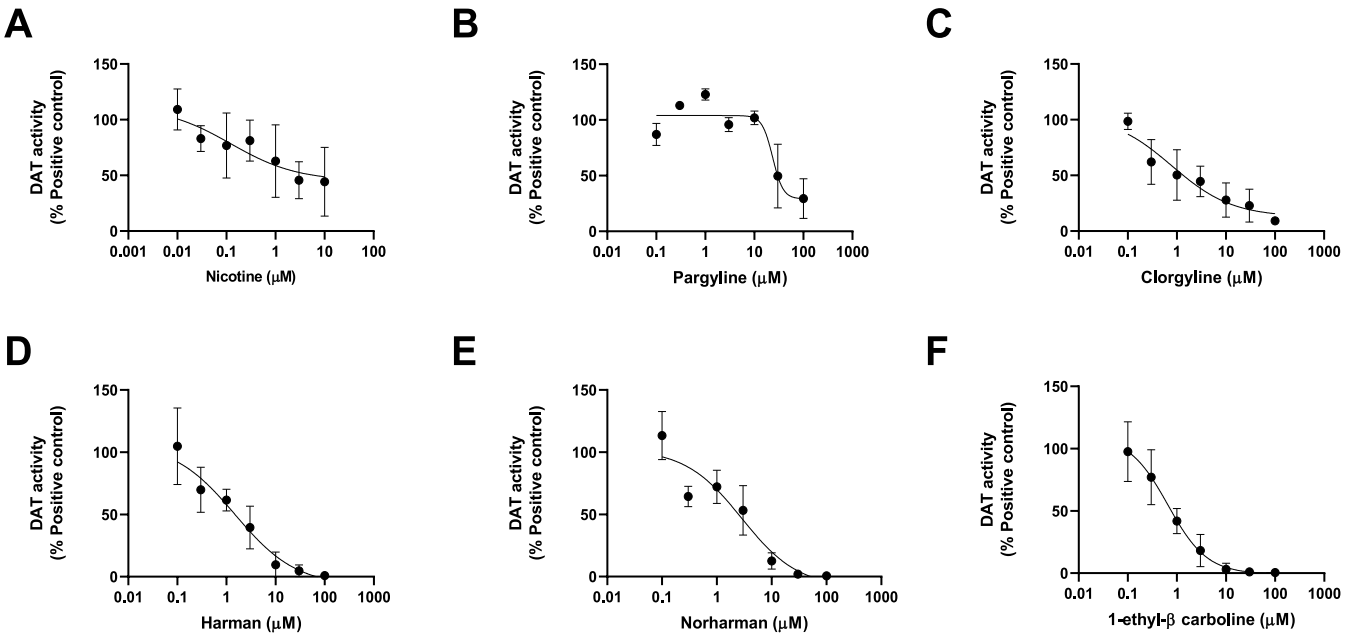


**Figure 3.** MAO-A inhibitors dose-dependently reduce DAT activity *in vitro*. Effects of (A) nicotine, (B) pargyline, (C) clorgyline, (D) harman, (E) norharman, and (F) 1-ethyl-$\beta$ carboline on DAT activity. Tested compounds show reduction in DAT activity and consequent fluorescent dye uptake at low micromolar doses except for pargyline, which results in being effective at concentrations higher than 10 $\mu$M. Data are presented as mean ± standard deviation, $n \geq 3$.

initial loading via DAT, which was in line with our hypothesis. Interestingly, synaptosomes pretreated with the nonspecific MAO-A/MAO-B inhibitor norharman still released a considerable fraction of [$^3$H] dopamine with the application of 30 mM KCl, possibly due to a partial inhibition of the loading, which would need verification in a dedicated study. Filters with trapped synaptosomes were measured for residual radioactivity and expressed in counts per minute, showing that synaptosomes treated with all MAO-AIs had significantly lower [$^3$H] dopamine, confirming the impaired loading with the pretreatments. This effect was comparable to that of synaptosomes treated with 10 $\mu$M nomifensine, which prevented [$^3$H] dopamine loading (Figure S4).

**Selected MAO-A Inhibitors Induce Marked [$^3$H] Dopamine Release from Rat Striatal Synaptosomes Including 1-Ethyl-$\beta$-carboline: A Newly Identified MAO-A Inhibitor from Tobacco Smoke.** After assessing the effects of MAOIs in direct MAO enzymatic inhibition, in direct DAT transport inhibition, and in a synaptosomal system, we next asked whether these compounds directly mediate dopamine release. To investigate this effect, synaptosomes were incubated with [$^3$H] dopamine, allowed to equilibrate to remove nonspecific [$^3$H] dopamine leaks, and then treated with three sequential stimuli: 100 $\mu$M MAOIs alone, 1 $\mu$M nicotine in the presence of 100 $\mu$M MAOIs, and 30 mM KCl for full synaptosome depolarization (Figure 6A). [$^3$H] Dopamine release was strongly evoked by clorgyline, norharman, harmaline, and 1-ethyl-$\beta$-carboline but not by the MAO-B control pargyline at the same concentration (Figure 6B). Nicotine-evoked [$^3$H] dopamine release was low in the presence of MAO-AIs, suggesting that these compounds had already depleted the synaptosome stores during the first stimulation (Figure 6C). A final 30 mM KCl-triggered depolarization was measured to assess any remaining [$^3$H] dopamine (Figure 6D). Filters containing trapped synaptosomes were finally analyzed after the three stimuli to detect residual radioactivity expressed in counts per minute and showed that synaptosomes treated with clorgyline, harmaline, and 1-ethyl-$\beta$-carboline contained less [$^3$H] dopamine compared with untreated synaptosomes, with harmaline being significantly lower than vehicle control (Figure S5). This observation confirms that MAO-AIs were able to trigger [$^3$H] dopamine release and empty the synaptosomes almost completely.

In this study, we focused on the effects of MAOIs contained in tobacco on the dopaminergic balance. Using a pharmacophore descriptor approach, we first found 12 tobacco-derived MAOIs, four of which inhibit the activity of the human MAO-A enzyme, while only one compound was found to inhibit the enzymatic activity of both human MAO-A and MAO-B. The compounds identified here as MAOIs are alkaloids belonging to the family of the $\beta$-carbolines and are already known MAOIs. This family of biologically active compounds occurs as indole derivatives with the core structure 9H-pyrido[3,4-*b*] indole, which represents the most basic $\beta$-carboline, namely norharman. Numerous $\beta$-carbolines analogues have been already described, and a comprehensive review of the different structure−activity relationship studies on $\beta$-carboline and its analogues was recently published.[29] Among the compounds identified during this study, harman, norharman, and harmaline had already been investigated for their inhibitory properties on MAO enzymes.[46−50] In contrast, 1-ethyl-$\beta$-carboline was, to the best of our knowledge, studied only once in 1968 in an investigation where different synthesized tetrahydro- and aromatic $\beta$-carbolines were assessed for their inhibitory activity on MAO.[27] In the context of CS, harman and norharman are, to date, the only $\beta$-carbolines investigated or cited as potent MAOIs found in tobacco smoke.[9,30−33] Nevertheless, it is known that CS contains numerous $\beta$-carbolines such as harmaline and 1-ethyl-$\beta$-carboline, which were both included in this study.[26,34] Additional $\beta$-carbolines were also identified, but their concentrations in CS have not


https://doi.org/10.1021/acschemneuro.4c00789
ACS Chem. Neurosci. 2025, 16, 1117−1131

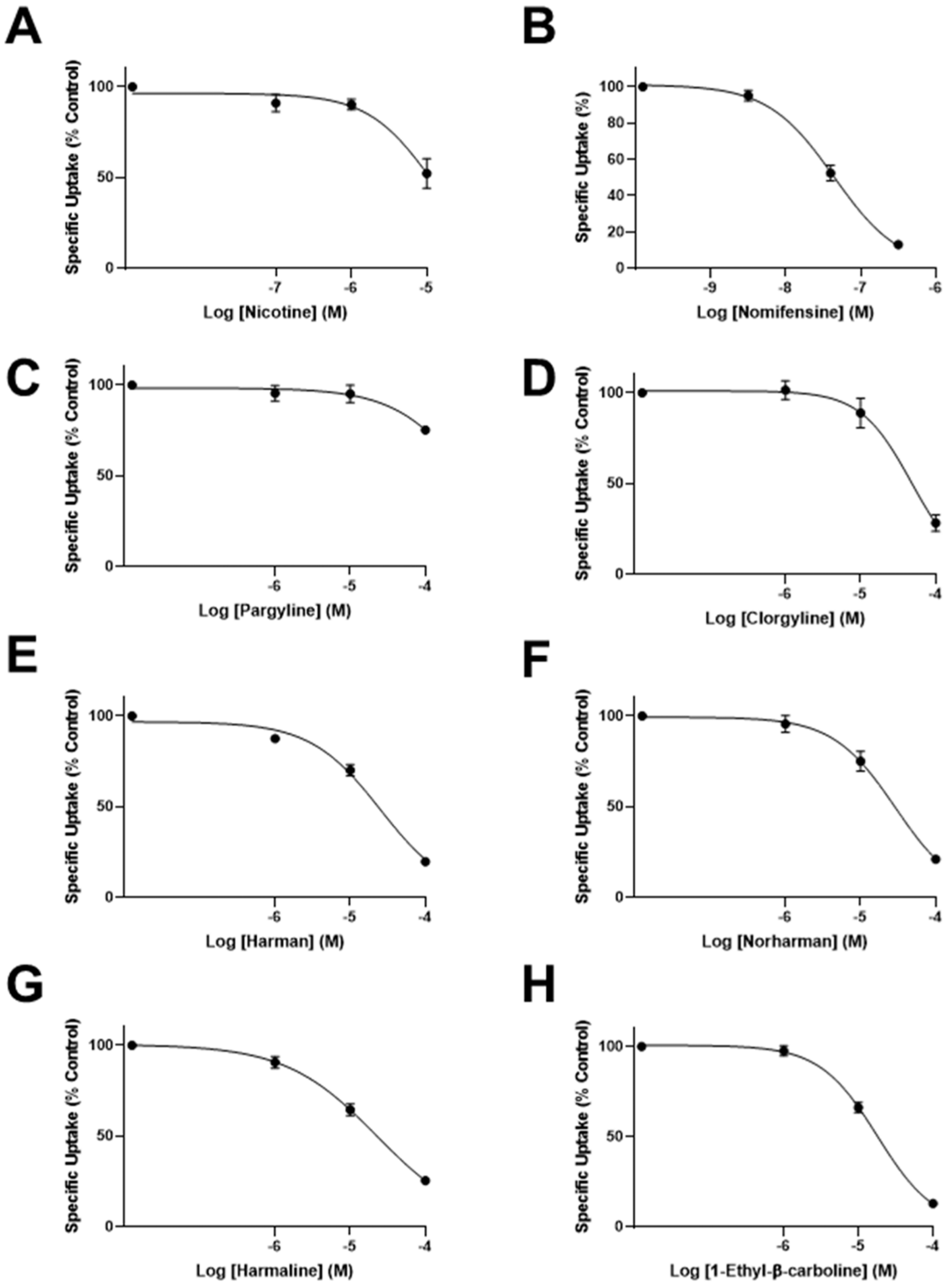


**Figure 4.** Effects of nicotine and MAOIs in [$^3$H] dopamine uptake in rat striatal synaptosomes. Four doses were tested for (A) nicotine, (B) nomifensine, (C) pargyline, (D) clorgyline, (E) harman, (F) norharman, (G) harmaline, and (H) 1-ethyl-$\beta$-carboline. All tested compounds reduced [$^3$H] dopamine reuptake by at least 50% except for pargyline. Data are presented as the mean ± standard error of the mean, $n$ = 3.

been determined yet. Among those, there are 1-butyl-$\beta$-carboline, 6-methoxy-1-methyl-$\beta$-carboline (isoharmine), 7-methoxy-1-methyl-$\beta$-carboline (harmine), 1-(1-propenyl)-$\beta$-carboline or *N*-methyl-$\beta$-carboline-3-carboxamide.[34] In addition, a recent publication evaluated mixed tobacco MAOIs, hydroquinones, and polyunsaturated fatty acids in animal behavioral tests relevant to nicotine addiction. The study found that the combined effects of tobacco MAOIs could enhance addictive responses to nicotine in rats. Conversely, no evidence of addictiveness was observed for these MAOIs when tested without nicotine.[35]


https://doi.org/10.1021/acschemneuro.4c00789
ACS Chem. Neurosci. 2025, 16, 1117−1131

**Table 4. $IC_{50}$ Values for Dopamine Uptake in Rat Striatal Synaptosomes**[a]

| compound name | MAO-A inhibition | MAO-B inhibition | uptake inhibition $IC_{50}$ [$\mu$M] |
|---|---|---|---|
| nomifensine (DAT control) | no | no | 0.044 |
| nicotine | no | no | 11.9 |
| 1-ethyl-$\beta$-carboline | yes | no | 18.0 |
| harmaline | yes | no | 22.5 |
| harman | yes | no | 25.4 |
| norharman | yes | yes | 29.0 |
| clorgyline (MAO-A control) | yes | no | 43.3 |
| pargyline (MAO-B control) | no | yes | 384.6 |

[a]DAT: dopamine transporter; $IC_{50}$: half-maximal inhibition; MAO: monoamine oxidase.

Our *in silico* analysis revealed a group of tobacco-derived MAOIs that are predicted to cross the BBB. The naturally occurring $\beta$-carboline, harman, was experimentally tested for BBB penetration and it was found, both in *ex vivo* experiments and *in vivo* in rats via receptor autoradiography, that this process occurs through an active uptake mechanism.[36−38] [$^3$H] harman was detected after intravenous administration in both blood and brain, at 25 and 30 min, respectively. Interestingly, [$^3$H] harman concentration was quite homogeneous in different brain regions upon systemic injection.[36] Pharmacokinetic studies were performed in the 1970s for several $\beta$-carbolines, such as harman, harmine, harmaline, and harmalol. Mice injected with these compounds showed heterogeneous brain concentrations over time as well as different elimination rates and plasma binding.[39,40] These data suggest that despite sharing chemical similarities, different $\beta$-carbolines have different pharmacokinetic properties. Further pharmacokinetics, stability, and plasma binding studies will be insightful

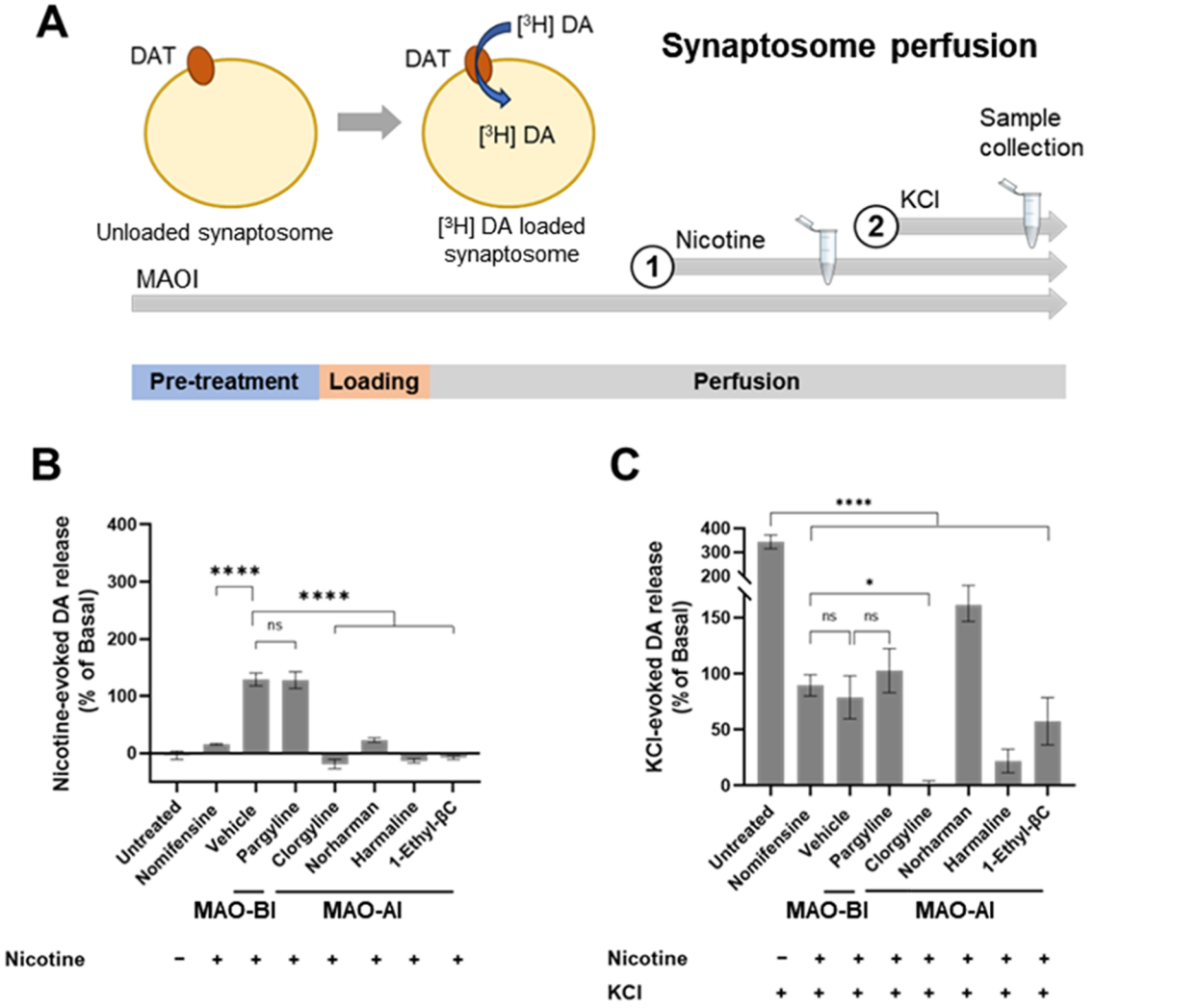


**Figure 5.** MAOIs strongly reduce [$^3$H] dopamine loading in synaptosomes. (A) Schematic representation of the stimulation sequence. (B) Synaptosomes, pretreated with MAOIs before [$^3$H] dopamine loading, were stimulated with 1 $\mu$M nicotine. MAOIs were present throughout the experiment. Nicotine-evoked [$^3$H] dopamine release was measured. All MAOIs except for pargyline blocked synaptosome loading, resulting in poor release. (C) (30 mM) KCl was finally added to induce full depolarization. Data are presented as mean ± standard error of the mean, $n$ = 3. Significance (*: $P$-value <0.05; ****: $P$-value <0.0001) was determined by one-way ANOVA and Dunnett's posthoc test. Abbreviations: DA, dopamine; DAT, dopamine transporter; 1-Ethyl-$\beta$C, 1-ethyl-$\beta$-carboline; MAO-AI, monoamine oxidase A inhibitor; MAO-BI, monoamine oxidase B inhibitor; ns, not significant.


https://doi.org/10.1021/acschemneuro.4c00789
ACS Chem. Neurosci. 2025, 16, 1117−1131

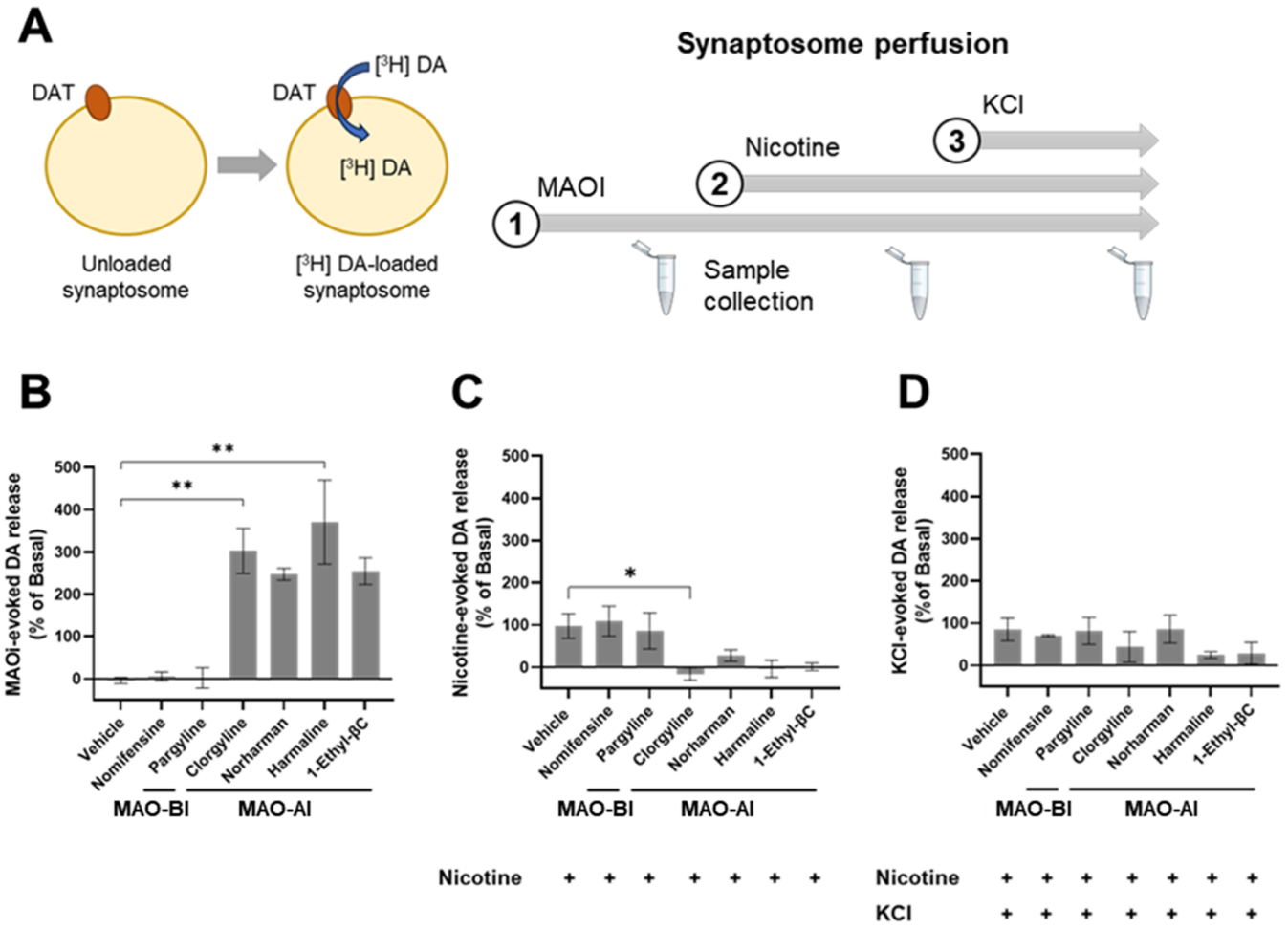


**Figure 6.** MAOIs strongly reduce [$^3$H] dopamine release in synaptosomes. (A) Schematic representation of the stimulation sequence. (B) Synaptosomes were loaded with [$^3$H] dopamine and treated in sequence with 100 $\mu$M of different MAOIs alone, (C) then concomitantly treated with 1 $\mu$M nicotine, and (D) finally treated with 30 mM KCl for full depolarization. All MAOIs, except for pargyline, triggered a strong [$^3$H] dopamine release before nicotine stimulation compared to the vehicle control. Data are presented as mean ± standard error of the mean, $n$ = 3. Significance (*: $P$-value <0.05; **: $P$-value <0.01) was determined by one-way ANOVA and Dunnett's posthoc test. Abbreviations: DA, dopamine; 1-Ethyl-$\beta$C, 1-ethyl-$\beta$-carboline; MAO-AI, monoamine oxidase A inhibitor; MAO-BI, monoamine oxidase B inhibitor.

to further clarify the properties of the newly identified 1-ethyl-$\beta$-carboline.

Truman and colleagues showed that harman and norharman might contribute to only 10% of the total MAO-A inhibition by CS,[41] suggesting that additional compounds are likely involved.[9] Based on these findings, it seems reasonable to postulate that other MAOIs such as harmaline and 1-ethyl-$\beta$-carboline may be relevant for MAO-A inhibition in the context of CS, based on their potency measured in this study with the MAO enzymatic assay (harmaline: $IC_{50}$ 23 nM; 1-ethyl-$\beta$-carboline: $IC_{50}$ 1.691 $\mu$M) and their concentration in CS (harmaline: 61.16 $\mu$g/item; 1-ethyl-$\beta$-carboline: 12.12 $\mu$g/item[26]).

In addition to their ability to directly inhibit MAO enzymes, we investigated the processes regulating dopamine balance at the synaptic level by analyzing both [$^3$H] dopamine release and uptake in rat striatal synaptosomes and an hDAT-CHO cell line. We showed that [$^3$H] dopamine release and uptake are influenced by MAOIs harman, norharman, 1-ethyl-$\beta$-carboline, and harmaline. In our compound selection, we observed that the MAO-AIs, but not the MAO-BI pargyline, significantly inhibited DAT activity, suggesting a specific role for the tested MAOIs in regulating dopamine uptake. The nonselective MAO-A/MAO-B norharman displayed a slightly weaker effect in both [$^3$H] dopamine release and uptake assays compared to specific MAO-AIs. This evidence is in line with a previous investigation where *in vivo* voltammetry and fluorescence imaging experiments demonstrated that MAO-A is the key contributor to the degradation of dopamine in the striatum, whereas MAO-B is more crucial in astrocytic $\gamma$-aminobutyric acid (GABA)-mediated tonic inhibition.[42] Additional studies on selective MAO-BIs are needed to confirm this observation.

Among the tested compounds, we have identified an MAO-AI derived from tobacco, 1-ethyl-$\beta$-carboline, to be a potent dopamine uptake inhibitor both *in vitro* and *ex vivo* and stimulates a strong dopamine release *ex vivo*. Our data suggest that 1-ethyl-$\beta$-carboline might be an additional contributor to the reward pathway by increasing and/or prolonging dopamine accumulation extracellularly, which, to the best of our knowledge, was not documented before. Similarly, harmaline has been reported to induce [$^3$H] dopamine release in rat striatal slices at both 58.3 and 5.83 $\mu$M concentrations,[24] in line with our observations in synaptosomes derived from the same brain region, even though at higher concentration (100 $\mu$M). Additionally, we found for the first time that harmaline reduces [$^3$H] dopamine uptake with a 22.5 $\mu$M $IC_{50}$ value. Our


https://doi.org/10.1021/acschemneuro.4c00789
ACS Chem. Neurosci. 2025, 16, 1117−1131

choice to test a relatively high concentration of a compound for [$^3$H] dopamine release stimulation in rat striatal synaptosomes was driven by the need to elicit a quantifiable [$^3$H] dopamine release in a complex perfusion system. This is not uncommon in this type of experiment. In fact, 200 $\mu$M harmine was reported as an effective dose in a [$^3$H] dopamine release assay in striatal slices, as lower concentrations were not sufficient to trigger a quantifiable response.[24]

Another important aspect to consider is the choice of multispecies models in this study. We show that our human enzyme *in vitro* analysis confirmed the results obtained in rat striatal synaptosomes with a factor of approximately 10-fold higher potency for the tested MAOIs. The increased potency is likely due to the higher sensitivity of the cellular system seen in hDAT-CHO cells, as well as to the different kinetics between hDAT constitutively expressed in CHO cells and rat DAT endogenously expressed in synaptosomes.[43] Since DAT has been studied in a variety of *in vitro* and *in vivo* models, it is crucial to be aware of the variations that different systems imply. For example, it has been reported that the human DAT constitutively expressed in cell lines has a $V_{max}$ ranging from 1 to 15.7 pmol/min/$10^5$ cells and a $K_m$ between 0.7 and 2.2 $\mu$M. In contrast, DAT expressed in rat striatal synaptosomes display a $V_{max}$ between 6 and 159 pmol/min/mg and a $K_m$ between 0.03 and 0.5 $\mu$M.[43] These differences might depend on DAT's various conformational states. For example, the outward conformation that binds extracellular dopamine, the occluded forms controlled by intra- and extracellular gates regulating the direction of the transport, the inward transporter conformations that release dopamine intracellularly, and the reorientation of the "empty" transporter back to the outward state, which allows it to start another cycle of transport.[5] Furthermore, these events are finely controlled by other molecular regulators (e.g., syntaxin 1A, flotillin 1, dopaminergic receptors, and G protein subunits), post-translational modifications (e.g., phosphorylation, glycosylation, and palmitoylation), cholesterol content, and membrane raft partitioning which obviously differ between brain preparations and cellular systems.[43] This set of differences might also explain why we observed a reduction in [$^3$H] dopamine uptake in rat striatal synaptosomes but not in hDAT-CHO cells.

Behavioral studies have hypothesized that nicotine influences reward-based decision-making in humans via DAT, probably by reducing DAT expression with a consequent impact on the extracellular dopamine concentration.[43] Moreover, nicotine may act as a stimulating molecule by reducing DAT activity in the striatum resulting in increased dopamine levels at synapses, as recently observed by Wang and colleagues in a clinical study.[44] Although the underlying mechanism is not fully clear, we can speculate that nicotine interacts with the extracellular portion of DAT and changes its conformation in the brain, causing a deceleration in the reuptake phase (direct effect). Alternatively, nicotine might initiate intracellular signal transduction processes that reduce DAT expression, with an impact on both the activity and the reuptake at the presynaptic level (indirect effect).

An important aspect to highlight is the mechanism of action by which MAO-AIs trigger dopamine release independently of binding, activating, or modulating nicotinic receptors. There is evidence that several $\beta$-carbolines such as harmaline, harmine, and other analogs—with higher affinity in the pyridyl-unsaturated form rather than the saturated one—bind serotoninergic receptors 5-$HT_{2A}$ and 5-$HT_{2C}$ in radioligand binding studies.[45−47] Additionally, $\beta$-carbolines bind the benzodiazepine site on the $GABA_A$ receptor but binding in a more physiological system has not been tested yet to the best of our knowledge.[24,45] An alternative mechanism of action for MAOIs on dopamine uptake might be that MAOIs/$\beta$-carbolines are transported through the DAT rather than directly binding it and their transport might compete with dopamine transport. This speculation would be supported by our competition experiment with native dopamine and the fluorescent dye mimicking dopamine, where we detect decreasing intracellular fluorescence with increasing native dopamine concentrations (Figure 2A). Current experimental setups do not allow for a deeper understanding of this phenomenon, which requires further investigation.

Given the broad-spectrum activity of MAOIs, off-target effects on other enzymes and receptors must be carefully considered as they might significantly influence dopamine dynamics. Notably, MAOIs interact with both MAO-A and MAO-B enzymes, leading to increased levels of not only dopamine but also serotonin and norepinephrine, which may further alter neurotransmission. Additionally, increased dopamine levels affect catechol-*O*-methyltransferase (COMT) activity, highlighting the interconnected nature of neurotransmitter metabolism. Some MAOIs can elevate serotonin levels, which, in turn, can influence dopamine dynamics due to the intricate interplay between serotonin and dopamine systems. The MAOI tranylcypromine has been observed to increase serotonin levels, which can affect mood and anxiety disorders. Elevated norepinephrine levels from MAO inhibition impact adrenergic receptors, affecting dopamine release and reuptake, while the potential for tyramine interaction poses a critical safety concern, emphasizing the need for dietary restrictions and patient education.[48] This crosstalk between neurotransmitter systems necessitates a nuanced approach *in vivo* and in medical treatments, particularly in patients with comorbid conditions involving both serotonin and dopamine dysregulation. These interactions underscore the complexity of using MAOIs and the necessity for careful management to optimize therapeutic outcomes while minimizing adverse effects.

Taken together, our data show the biological effects of four MAOIs on dopamine neurotransmission: harman, norharman (well-documented in previous literature), harmaline, and 1-ethyl-$\beta$-carboline (previously less explored). The tested MAOIs have three effects: (i) direct MAO inhibition by preventing the degradation of neurotransmitters by blocking MAO enzyme activity, (ii) DAT activity inhibition by preventing or reducing the reuptake of the neurotransmitters from the synaptic cleft, and (iii) induction of dopamine release from the presynaptic terminal into the synaptic cleft. This work provides updated and detailed knowledge on the specific actions of MAO-AIs, which are not strictly linked to MAO only but involve DAT as well as dopamine release and uptake. This collective evidence underscores the significance of both MAO and DAT as targets for a comprehensive mechanistic understanding of the effects of nicotine and MAOIs in the context of dopamine neurotransmission, although they are not unique components of a multifaceted phenomenon.

Further studies should investigate the potential effects of less explored MAOIs on the neurotransmitter balance. One possible approach is to test 1-ethyl-$\beta$-carboline (and potentially other novel MAOIs) *in vivo* using real-time techniques to directly measure MAOIs effects on neurotransmitter release


https://doi.org/10.1021/acschemneuro.4c00789
ACS Chem. Neurosci. 2025, 16, 1117−1131

Table 5. List of Used Compounds[a]

| compound name | mode of action | molecule type | supplier | CAS no. |
|---|---|---|---|---|
| nicotine | nAChR agonist | alkaloid | Merck, Darmstadt, Germany | 54−11−5 |
| dopamine hydrochloride | neurotransmitter | phenylethylamine | Merck, Darmstadt, Germany | 62−31−7 |
| [$^3$H] dopamine | neurotransmitter | phenylethylamine | PerkinElmer, Waltham, MA | 18683−98−2 |
| harman | MAO-A/B inhibitor | alkaloid | Merck, Darmstadt, Germany | 486−84−0 |
| harmaline | MAO-A/B inhibitor | DH$\beta$C alkaloid | Merck, Darmstadt, Germany | 304−21−2 |
| norharman | MAO-A/B inhibitor | $\beta$C alkaloid | Merck, Darmstadt, Germany | 244−63−3 |
| clorgyline (R) | MAO-A inhibitor | aromatic amine | Merck, Darmstadt, Germany | 17780−75−5 |
| pargyline hydrochloride (R) | MAO-B inhibitor | aromatic amine | Merck, Darmstadt, Germany | 306−07−0 |
| nomifensine (R) | DA reuptake inhibitor | isoquinolin derivative | Tocris, Bristol, UK | 32795−47−4 |
| 1-ethyl-b-carboline | MAO-A inhibitor | $\beta$C alkaloid | Achemblock, Hayward, CA | 20127−61−1 |
| 5-cyanonicotine | N/A | nicotine derivative | WuXi AppTec, Shanghai, China | 42459−12−1 |
| 2-methyl-3-phenylpyrazine | N/A | pyrazine derivative | Sigma, St. Louis, MO | 29444−53−9 |
| nicotelline | N/A | alkaloid | Selvita, Kraków, Poland | 494−04−2 |
| myosmine | N/A | alkaloid | WuXi AppTec, Shanghai, China | 532−12−7 |
| 2,3′-bipyridyl | N/A | alkaloid | Sigma, St. Louis, MO | 581−50−0 |
| $N'$-nitrosoanatabine | N/A | nitrosamine | Supelco, Bellefonte, PA | 887407−16−1 |
| 2,2′-bipyridyl | N/A | alkaloid | Sigma, St. Louis, MO | 366−18−7 |
| anatabine cytrate | nAChR agonist | alkaloid | WuXi AppTec, Shanghai, China | 1335287−69−8 |
| M30 dihydrochloride | MAO-A inhibitor | hydroxyquinoline derivative | Sigma, St. Louis, MO | 64821−19−8 |

[a]Abbreviations: DA: dopamine; MAO: monoamine oxidase; nAChR: nicotinic acetylcholine receptor; N/A: not applicable.

and metabolism in specific brain regions. Additionally, behavioral tests would be beneficial to assess anxiety-like states, substance dependence, and neuroprotection.[49] These approaches hold promise for shedding light on the molecular intricacies of dopaminergic signaling in the context of the reward system.

## METHODS

**Description of MAO Inhibitors and Tobacco Compounds Data sets.** To identify potential MAOIs via an *in silico* pharmacophore-based approach, the following data sets were used: (i) data sets of known MAOIs and corresponding $IC_{50}$ values compiled by Kumar et al.[50] and based on recently published MAO-AIs ($N$ = 1546 MAO-AIs with $IC_{50}$ values ranging between 0.000418 and 98.49 $\mu$M) and MAO-BIs ($N$ = 2177 MAO-BIs with $IC_{50}$ values ranging between 0.00021 and 98 $\mu$M); (ii) the binding database[51−53] to retrieve already reported MAOIs, and (iii) a data set of tobacco compounds ($N$ = 485 identified compounds) extracted from Bentley et al.[26]

**Pharmacophore Model and Molecular Docking.** To compare the pharmacophore similarity among known MAOIs and tobacco compounds, the compounds were encoded using pharmacophore descriptors.[54] DataWarrior software (open source)[55] was used to calculate the pharmacophore descriptors and perform the pharmacophore similarity comparison. The similarity threshold to consider a compound as a potential MAOI was set to 85%. The crystal structures of human MAO-A (PDB ID 2Z5X)[56,57] and MAO-B (PDB ID 2V5Z)[58,59] were retrieved from the Protein Data Bank.[60] The Molecular Operating Environment (MOE, Montreal, Quebec, Canada) software version 2020.09[61] was used to perform the molecular docking simulations. The dominant protonation state at pH 7.4 of the compounds to be docked (compounds selected in previous steps as potential MAOIs) was determined using the ChemAxon Major Microspecies Plugin (ChemAxon, Budapest, Hungary).[61] The orthosteric sites of each crystal structure for the docking simulation were identified around the cocrystallized ligands. The "triangle matcher" function was selected as the placement method, and the London -G was selected as the scoring function, which estimates the free energy of binding of the ligand from a pose, knowing that the lowest -G values correspond to the highest binding affinity. The best poses were refined and rescored using the Generalized Born Volume Integral/Weighted Surface Area (GBVI/WSA) -G score and the binding energy value extracted from the best pose. The GBVI/WSA -G is a force field-based scoring function, which estimates the free energy of binding of the ligand from a given pose.[62] The calculated binding affinities were analyzed and compared with known cocrystallized ligands.

***In Silico* Blood−Brain-Barrier (BBB) Permeability Prediction.** For *in silico* BBB permeability prediction, the admetSAR and BIOVIA ADMET Blood Brain Barrier Models were used.

*AdmetSAR Model.* The admetSAR (v2.0) server was used to predict the chemical absorption, distribution, metabolism, excretion, and toxicity (ADMET) parameters of the candidate compounds. The BBB model was developed using a data set derived from the work of Shen et al., including 1839 compounds (1438 BBB-permeable and 401 BBB-impermeable compounds).[63] Values equal to or close to 1 indicated compounds with a high probability of BBB penetration.

*BIOVIA ADMET BBB Model.* The BIOVIA ADMET BBB Model was used as an additional tool to predict the BBB penetration of a molecule, defined as the ratio of concentrations (brain concentration/blood concentration) after oral administration, and to report the predicted penetration as well as a classification of the penetration level. The model combined a confidence ellipse in the polar surface area and LogP descriptor space, derived from over 800 orally administered compounds classified as CNS therapeutics with a robust regression model based on 120 compounds with measured penetration to predict Log (brain blood (BB)) penetration values for those molecules falling within the confidence ellipse.[64] The model predicted the BB permeation level based on the categories "very high" (BB ratio >5:1), "high" (BB between 1:1 and 5:1), "medium" (BB between 0.3:1 and 1:1), "low" (<0.3:1), and "undefined" (outside the 99% confidence range ellipse). This translates into the regression model prediction values of Log (BB) > 0.7 for "very high", 0 < Log (BB) < 0.7 for "high", −0.52 < Log (BB) < 0 for "medium", and Log (BB) < −0.52 for "low." No prediction was made for compounds outside the 95% confidence ellipsoids.

**Chemicals.** Compound chemicals were purchased from commercial suppliers and are listed in Table 5. Compounds were prepared in dimethyl sulfoxide (DMSO, Sigma-Aldrich, St. Louis, MO) and stored at −80 °C.

**MAO Enzymatic Assay.** The two-step MAO-Glo bioluminescent assay (Promega, Madison, WI) was performed according to the manufacturer's instructions and as described elsewhere.[65] Human recombinant MAO (MAO-A and MAO-B, 0.4 and 0.1 U/well of microsomal protein, respectively) were incubated with a derivative of


https://doi.org/10.1021/acschemneuro.4c00789
ACS Chem. Neurosci. 2025, 16, 1117−1131

beetle luciferin ((4S)-4,5-dihydro-2-(6-hydroxybenzothiazolyl)-4-thiazolecarboxylic acid) substrate and sample/vehicle for 1 h at room temperature in a 50-μL-reaction mixture. The beetle luciferin substrate concentrations were varied for determining the kinetic constants, but all subsequent experiments used the substrate at the Michaelis constant (Km) values of 20 and 3 μM (MAO-A and MAO-B, respectively). In the luciferin detection reaction, 50 μL of the luciferin detection reagent (Promega, Madison, WI) was added to the MAO reaction. After a 1 h incubation period, the luminescent signal was measured by using a Fluostar Omega 96 Microplate reader (BMG LABTECH GmbH, Ortenberg, Germany).

**Cell Culture.** Chinese hamster ovary (CHO) cell lines constitutively expressing human DAT (hDAT; GenBank accession number NM_001044) were obtained from BPS Bioscience (San Diego, CA). Cells were maintained in DMEM/F12 medium (Gibco, Thermo Fisher Scientific, Waltham, MA) supplemented with 10% heat-inactivated fetal bovine serum (Gibco) and penicillin-streptomycin (100 U/mL and 0.1 mg/mL, respectively) solution (Sigma-Aldrich, St. Louis, MO) at 37 °C in 5% $CO_2$. The hDAT-CHO cells were continuously cultured in the presence of hygromycin (0.4 mg/mL, InvivoGen, San Diego, CA) according to manufacturer protocols. For the *in vitro* neurotransmitter uptake assay, cells were seeded in 96-well plates, black walls clear bottom (Costar, Corning, NY) for 24 h at 37 °C in 5% $CO_2$ at cell density between 10 and 20,000 cells per well in 100 μL cultivation medium.

**Neurotransmitter Uptake and DAT Activity Assay.** The DAT activity assay was performed using the Neurotransmitter transporter uptake assay kit[66,67] (Cat. R8174 from Molecular Devices, Sunnyvale, CA). For hDAT-CHO cells pretreatment, cultivation medium was removed and replaced by the HBPS buffer made of Hank's Balanced Salt Solution (HBSS), containing 138 mM NaCl, 5.3 mM KCl, 0.9 mM $MgCl_2$, 1.2 mM $CaCl_2$, 5.5 mM glucose, (Gibco) and 10 mM (4-(2-hydroxyethyl)-1-piperazineethanesulfonic acid (HEPES)) at pH 7.4 (Gibco), 90 μL per well. Compounds prepared in DMSO (Sigma-Aldrich) were diluted to obtain 1:3 serial dilutions and then further diluted in HBPS at 10× the final concentration. hDAT-CHO cells were pretreated by adding 10 μL compound solution (10×) in 90 μL HBPS buffer to reach the final concentration and incubated for 15 min at 37 °C and 5% $CO_2$. The pretreatment was replaced with a fluorescent dye containing the compounds for 30 min to ensure constant inhibition of the dye uptake. At the end of the incubation time, nuclear staining solution with Hoechst 33342, 10 mg/mL solution in water (Thermo Fisher, Waltham, MA) was prepared in HBPS at 1:1000 final dilution onto the cells and incubated for 10 min.

The fluorescent signal was analyzed by high-content screening Thermo CellInsight CX7 (Thermo Fisher) in hDAT-CHO cells incubated with the fluorescent dye. In a 96-well plate, 9 fields of view per well were acquired at 10× magnification. Both the positive and negative control wells were used to set up the acquisition parameters. First, the 350 nm (Hoechst) channel was adjusted to have a 50% signal intensity. Multiple wells were used as a reference, and the exposure was adapted to match these criteria consistently in all of the wells. Second, the 488 nm (GFP) signal was adjusted to 70 to 80% fluorescence in the positive control wells containing the dye only and vehicle HBPS, and 5 to 10% in the negative control wells (no dye present), considered as the background signal. Then, all wells were acquired with the selected parameters, and the GFP fluorescence was normalized to the positive control that was considered as 100%.

**Rat Striatal Synaptosome Preparation.** Adult male Sprague–Dawley rats (200–225 g body weight) were purchased from Charles River UK, Ltd. (Kent, United Kingdom) and were housed at the University of Birmingham animal facility, which has a procedure establishment license issued by the Secretary of State and conforms to all relevant United Kingdom legislation. The animals were managed by Gifford Bioscience and terminated in accordance with schedule one procedures issued by the UK home office. For both [$^3$H] dopamine release and uptake assays, freshly dissected rat striatal tissue was added to sucrose buffer (0.32 M sucrose), homogenized with a Dounce homogenizer, and centrifuged at 100*g* to remove cell's debris. The supernatant was collected and centrifuged 17,000*g* for 10 min at 4 °C to pellet the synaptosomes. The pellet was resuspended in the fresh Krebs assay buffer at pH 7.4 containing 120 mM NaCl, 3.3 mM KCl, 1.2 mM $MgSO_4$, 1.3 mM $CaCl_2$, 1.2 mM $K_2HPO_4$, 25 mM HEPES, 11 mM glucose, and 0.01 mM ascorbic acid.

**[$^3$H] Dopamine Uptake Assay in Rat Striatal Synaptosomes.** The compounds listed in Table 5 were dissolved in DMSO (10 or 20 mM) and stored at −20 °C. On the day of the assay, compounds were thawed and diluted with the assay buffer to 5× final maximal assay concentration. Uptake assays were carried out in 96-well plates in a final volume of 250 μL per well. A volume of 50 μL of test compound, nonspecific compound, or vehicle was added to each well containing 150 μL of rat striatal synaptosomes preparation. The plate was incubated at 25 °C for 10 min with gentle agitation. Next, 50 μL radiolabeled [$^3$H] dopamine (PerkinElmer, Shelton, CT) was added to each well to initiate the dopamine uptake. The plate was incubated at 25 °C for a further 4 min with gentle agitation. The incubation was stopped by vacuum filtration onto presoaked GF/C filters using a 96-well FilterMate harvester, followed by 3 washes with ice-cold wash buffer. Filters were then dried under a warm air stream and sealed in polyethylene; scintillation cocktail was added, and the radioactivity was counted in a Wallac TriLux 1450 MicroBeta counter (Wallac Oy, Turku, Finland).

**[$^3$H] Dopamine Release Assay in Rat Striatal Synaptosomes.** *[$^3$H] Dopamine Loading Protocol.* For pretreatment, the synaptosomal pellet was resuspended in the Krebs buffer containing the MAOIs and test compounds other than nicotine at their final assay concentration and incubated for 15 min at 35 °C with gentle shaking. Then, [$^3$H] dopamine was added to a final concentration of 1 μCi/mL, and the synaptosomes were incubated for a further 15 min at 35 °C with gentle shaking. Following incubation, synaptosomes were loaded onto GF/C filters contained in filter chambers and placed in a superfusion system. The preoxygenated Krebs buffer containing the compounds at the final assay concentration was perfused through the chambers at a rate of 1 mL/min at 35 °C using a peristaltic pump. Trapped air bubbles were removed from the filters prior to collecting fractions to ensure an even flow over the synaptosomal bed. After a superfusion period of 60 min, 2 basal fractions (2 mL/fraction at 1.5 mL/min) were collected, followed by a further 3 fractions containing 1 μM nicotine. Finally, the high KCl (30 mM) Krebs buffer was added to evoke release, and a further 2 fractions were collected. Following collection, a 0.3 mL aliquot of each fraction was transferred to a counting plate, 0 6 mL scintillation cocktail was added, and radioactivity in the aliquot was counted using a Wallac TriLux 1450 MicroBeta (Wallac Oy) counter. Once all fractions had been collected, the filters holding the synaptosomes were removed, dried, scintillation cocktail added, and the filters counted to determine residual radioactivity.

*[$^3$H] Dopamine Release Protocol.* The synaptosomal pellet was resuspended in Krebs buffer containing 1 μCi/mL [$^3$H] dopamine and incubated for 15 min at 35 °C with gentle shaking. Following incubation, [$^3$H] dopamine-treated synaptosomes were loaded onto GF/C filters inside the filter chambers and placed in a superfusion system. The preoxygenated Krebs buffer was perfused through the chambers at a rate of 1 mL/min at 35 °C using a peristaltic pump. Trapped air bubbles were removed from the filters prior to collecting fractions to ensure an even flow over the synaptosomal bed. After a superfusion period of 60 min, 2 basal fractions (2 mL/fraction at 1.5 mL/min) were collected, followed by a further 3 fractions (2 mL/fraction at 1.5 mL/min) containing MAOIs or other compounds at their final assay concentrations. The compounds were perfused over the synaptosomes for a further 5 min to allow the response of the synaptosomes to normalize after the addition of the compounds. Two basal fractions were then collected (2 mL/fraction at 1.5 mL/min) followed by 3 fractions containing 1 μM nicotine in the presence of MAOIs or other compounds. Finally, the high KCl Krebs buffer (30 mM) was added to evoke release and a further 2 fractions were collected. Following collection, a 0.3 mL aliquot of each fraction was transferred to a counting plate, 0.6 mL scintillation cocktail was added, and radioactivity in the aliquot was counted using a Wallac TriLux 1450 MicroBeta (Wallac Oy) counter. Once all fractions had


https://doi.org/10.1021/acschemneuro.4c00789
ACS Chem. Neurosci. 2025, 16, 1117−1131

been collected, the filters holding the synaptosomes were removed, dried, scintillation cocktail added, and the filters counted to determine residual radioactivity.

**Data Analysis.** For the MAO enzymatic assay, chemiluminescent values, half-maximal inhibitory concentrations ($IC_{50}$), and 95% confidence interval were analyzed using Prism version 9 for Windows (GraphPad Software, Inc., San Diego, CA). Data are shown as mean ± standard error of the mean (SEM).

For cellular neurotransmitter uptake and DAT activity assay, images were analyzed by SpotDetector analysis. Plotted values correspond to the total intensity (MEAN_ObjectSpotTotalIntenCh2). Total intensity values were then normalized to the positive control corresponding to the maximal dye uptake in HBPS buffer only, which was considered as 100%. The normalized values were then used to build a 4-parameter Hill's equation in Prism9. Data are shown as the mean ± standard deviation (SD).

For the dopamine release assay, compound-evoked neurotransmitter release was calculated. The value counts per minute of two basal fractions collected immediately prior to compound addition were subtracted from the counts per minute values of two fractions collected immediately following compound application. The compound-evoked release was calculated as a percentage of the basal release from each chamber. The values were plotted in Prism9, presented as mean ± SEM. For dopamine uptake assay at each concentration of compound, nonspecific uptake was subtracted from total uptake to give specific uptake. Specific uptake was then normalized to the control wells each day. Data was fitted using the nonlinear curve fitting routines in Prism9 to determine $IC_{50}$ values. For all experiments, at least three replicates were performed over different experimental days.

## ■ ASSOCIATED CONTENT

### Data Availability Statement

The data that support the findings of this study are available from the corresponding author, G.S., upon reasonable request.

### Supporting Information

The Supporting Information is available free of charge at https://pubs.acs.org/doi/10.1021/acschemneuro.4c00789.

Figure S1: dose−response curves showing the effects of reference and test compounds on human MAO-A and -B in the *in vitro* enzymatic activity assay; Figure S2: comparison of 1-ethyl-β-carboline vs harmine docking poses within the orthosteric binding site of the MAO-A crystal structure. Figure S3: assessment of the specificity of the human DAT in the *in vitro* activity assay; Figure S4: quantification of the residual [$^3$H] dopamine detected in rat striatal synaptosomes after dopamine loading assessment; Figure S5: quantification of the residual [$^3$H] dopamine detected in rat striatal synaptosomes after dopamine release assessment (PDF)

## ■ AUTHOR INFORMATION


### Corresponding Author

**Gabriella Saro** − *PMI R&D, Philip Morris Products S.A., 2000 Neuchâtel, Switzerland;* orcid.org/0000-0003-4553-0024; Email: gabriella.saro@pmi.com

### Authors

**Stephanie Johne** − *PMI R&D, Philip Morris Products S.A., 2000 Neuchâtel, Switzerland*

**Diogo A.R.S. Latino** − *Rosa Serra Latino Consulting, 6300 Zug, Switzerland*

**Fabian Moine** − *PMI R&D, Philip Morris Products S.A., 2000 Neuchâtel, Switzerland*

**Marco van der Toorn** − *PMI R&D, Philip Morris Products S.A., 2000 Neuchâtel, Switzerland*

**Carole Mathis** − *PMI R&D, Philip Morris Products S.A., 2000 Neuchâtel, Switzerland*

**Emilija Veljkovic** − *PMI R&D, Philip Morris Products S.A., 2000 Neuchâtel, Switzerland*

Complete contact information is available at: https://pubs.acs.org/10.1021/acschemneuro.4c00789


### Author Contributions

G.S.: Conceptualization, methodology, validation, investigation, resources, data curation, formal analysis, visualization, writing—original draft, and writing—review and editing. S.J.: Methodology, validation, investigation, resources, data curation, formal analysis, and visualization. C.M.: Conceptualization, supervision, project administration, and writing—review and editing. F.M.: Conceptualization, formal analysis, visualization, writing—original draft, and writing—review and editing. D.A.R.S.L.: Methodology, validation, investigation, resources, data curation, formal analysis, visualization, and writing—original draft. M.v.d.T.: Conceptualization, supervision, project administration, methodology, and writing—review and editing. E.V.: Conceptualization, supervision, project administration, and writing—review and editing.

### Notes

The authors declare no competing financial interest.

Nicotine is known to stimulate the dopamine system in the human brain. However, other tobacco compounds also impact the dopamine balance. Using an *in silico* approach, tobacco components were screened to identify other, less-studied molecules with the potential to inhibit the monoamine oxidase (MAO) enzymes responsible for breaking down dopamine. Among the screened molecules, four were identified as MAO inhibitors (MAOIs). The four MAOIs were assessed for their ability to influence the dopamine transporter activity in a cellular system as well as dopamine release and uptake in synaptosomes (a preparation of synaptic terminals in brain cells). Interestingly, this study provides the first evidence of a new MAOI (1-ethyl-β-carboline) as a modulator of dopamine balance by stimulating dopamine release and reducing dopamine reuptake *in vitro*. This new finding expands the knowledge of the effects of nicotine and other tobacco compounds on the dopamine system and improves the current mechanistic understanding of biological processes relevant to reward pathway modulation.

## ■ ACKNOWLEDGMENTS

The authors would like to thank the Gifford Bioscience team (Birmingham, UK), especially Dr. Andrew Gifford and Dr. Sian Stockton for their invaluable technical and scientific expertise in synaptosome-based dopamine release and uptake experiments and data analysis. We are grateful to Athanasios Kondylis and Iris Legbre for their help in statistical analysis. This study was funded and sponsored by Philip Morris International.

## ■ ABBREVIATIONS

ADMET:absorption, distribution, metabolism, excretion, and toxicity
ANOVA:analysis of variance
BB:brain blood
BBB:blood−brain barrier

CAS:chemical abstracts service
CHO:Chinese hamster ovary
CS:cigarette smoke
CSE:cigarette smoke extract
COMT:cathecol-*O*-methyltransferase
DA:dopamine
DAT:dopamine transporter
Ethyl-$\beta$C:1-ethyl-$\beta$-carboline
GABA:$\gamma$-aminobutyric acid
GBVI/WSA:generalized born volume integral/weighted surface area
h:hour
HCS:high-content screening
hDAT:human dopamine transporter
$IC_{50}$:half-maximal inhibitory concentration
MAO:monoamine oxidase
MAO-A:monoamine oxidase type A
MAO-B:monoamine oxidase type B
MAOI:monoamine oxidase inhibitor
MAO-AI:monoamine oxidase type A inhibitor
MAO-BI:monoamine oxidase type B inhibitor
N/A:not applicable
NAc:nucleus accumbens
nAChR:nicotinic acetylcholine receptor
ns:not significant
SD:standard deviation
SEM:standard error of the mean
VTA:ventral tegmental area

## REFERENCES


(1) Tiwari, R. K.; Sharma, V.; Pandey, R. K.; Shukla, S. S. Nicotine Addiction: Neurobiology and Mechanism. *J. Pharmacopuncture* **2020**, *23* (1), 1−7.
(2) Dani, J. A.; De Biasi, M. Cellular mechanisms of nicotine addiction. *Pharmacol., Biochem. Behav.* **2001**, *70*, 439.
(3) Nestler, E. J. Is there a common molecular pathway for addiction? *Nat. Neurosci.* **2005**, *8* (11), 1445−1449.
(4) Zoli, M.; Pistillo, F.; Gotti, C. Diversity of native nicotinic receptor subtypes in mammalian brain. *Neuropharmacology* **2015**, *96*, 302−311, DOI: 10.1016/j.neuropharm.2014.11.003.
(5) Nepal, B.; Das, S.; Reith, M. E.; Kortagere, S. Overview of the structure and function of the dopamine transporter and its protein interactions. *Front. Physiol.* **2023**, *14*, No. 1150355.
(6) Jones, S. R.; Gainetdinov, R. R.; Jaber, M.; Giros, B.; Wightman, R. M.; Caron, M. G. Profound neuronal plasticity in response to inactivation of the dopamine transporter. *Proc. Natl. Acad. Sci. U.S.A.* **1998**, *95* (7), 4029−4034.
(7) Finberg, J. P. M.; Rabey, J. M. Inhibitors of MAO-A and MAO-B in Psychiatry and Neurology. *Front. Pharmacol.* **2016**, *7*, No. 340.
(8) Abuhamdah, S.; Khalil, A.; Sari, Y. Targeting Dopaminergic System for Treating Nicotine Dependence. *Cent. Nerv. Syst. Agents Med. Chem.* **2016**, *16* (2), 137−142.
(9) Hong, S. W.; Teesdale-Spittle, P.; Page, R.; Truman, P. A review of monoamine oxidase (MAO) inhibitors in tobacco or tobacco smoke. *Neurotoxicology* **2022**, *93*, 163−172.
(10) Truman, P.; Stanfill, S.; Heydari, A.; Silver, E.; Fowles, J. Monoamine oxidase inhibitory activity of flavoured e-cigarette liquids. *Neurotoxicology* **2019**, *75*, 123−128.
(11) Lewis, A.; Miller, J. H.; Lea, R. A. Monoamine oxidase and tobacco dependence. *Neurotoxicology* **2007**, *28*, 182−195.
(12) Hall, B. J.; Wells, C.; Allenby, C.; Lin, M. Y.; Hao, I.; Marshall, L.; Rose, J. E.; Levin, E. D. Differential effects of non-nicotine tobacco constituent compounds on nicotine self-administration in rats. *Pharmacol., Biochem. Behav.* **2014**, *120*, 103−108.
(13) Le Foll, B.; Piper, M. E.; Fowler, C. D.; Tonstad, S.; Bierut, L.; Lu, L.; Jha, P.; Hall, W. D. Tobacco and nicotine use. *Nat. Rev. Dis. Primers* **2022**, *8* (1), No. 19.
(14) Hong, S. W.; Teesdale-Spittle, P.; Page, R.; Ellenbroek, B.; Truman, P. Biologically Active Compounds Present in Tobacco Smoke: Potential Interactions Between Smoking and Mental Health. *Front. Neurosci.* **2022**, *16*, No. 885489.
(15) Sved, A. F.; Weeks, J. J.; Grace, A. A.; Smith, T. T.; Donny, E. C. Monoamine oxidase inhibition in cigarette smokers: From preclinical studies to tobacco product regulation. *Front. Neurosci.* **2022**, *16*, No. 886496.
(16) Smith, T. T.; Rupprecht, L. E.; Cwalina, S. N.; Onimus, M. J.; Murphy, S. E.; Donny, E. C.; Sved, A. F. Effects of Monoamine Oxidase Inhibition on the Reinforcing Properties of Low-Dose Nicotine. *Neuropsychopharmacology* **2016**, *41* (9), 2335−2343.
(17) Kim, H.; Sablin, S. O.; Ramsay, R. R. Inhibition of monoamine oxidase A by beta-carboline derivatives. *Arch. Biochem. Biophys.* **1997**, *337* (1), 137−142.
(18) Fowler, J. S.; Volkow, N. D.; Wang, G. J.; Pappas, N.; Logan, J.; Shea, C.; Alexoff, D.; MacGregor, R. R.; Schlyer, D. J.; Zezulkova, I.; Wolf, A. Brain monoamine oxidase A inhibition in cigarette smokers. *Proc. Natl. Acad. Sci. U.S.A.* **1996**, *93* (24), 14065−14069.
(19) Ding, Z.; Li, X.; Chen, H.; Hou, H.; Hu, Q. Harmane Potentiates Nicotine Reinforcement Through MAO-A Inhibition at the Dose Related to Cigarette Smoking. *Front. Mol. Neurosci.* **2022**, *15*, No. 925272.
(20) Smith, T. T.; Schaff, M. B.; Rupprecht, L. E.; Schassburger, R. L.; Buffalari, D. M.; Murphy, S. E.; Sved, A. F.; Donny, E. C. Effects of MAO inhibition and a combination of minor alkaloids, $\beta$-carbolines, and acetaldehyde on nicotine self-administration in adult male rats. *Drug Alcohol Depend.* **2015**, *155*, 243−252.
(21) Costello, M. R.; Reynaga, D. D.; Mojica, C. Y.; Zaveri, N. T.; Belluzzi, J. D.; Leslie, F. M. Comparison of the reinforcing properties of nicotine and cigarette smoke extract in rats. *Neuropsychopharmacology* **2014**, *39* (8), 1843−1851.
(22) Arnold, M. M.; Loughlin, S. E.; Belluzzi, J. D.; Leslie, F. M. Reinforcing and neural activating effects of norharmane, a non-nicotine tobacco constituent, alone and in combination with nicotine. *Neuropharmacology* **2014**, *85*, 293−304.
(23) Brierley, D. I.; Davidson, C. Harmine augments electrically evoked dopamine efflux in the nucleus accumbens shell. *J. Psychopharmacol.* **2013**, *27* (1), 98−108.
(24) Schwarz, M. J.; Houghton, P. J.; Rose, S.; Jenner, P.; Lees, A. D. Activities of extract and constituents of Banisteriopsis caapi relevant to parkinsonism. *Pharmacol., Biochem. Behav.* **2003**, *75* (3), 627−633.
(25) Drucker, G.; Raikoff, K.; Neafsey, E. J.; Collins, M. A. Dopamine uptake inhibitory capacities of beta-carboline and 3,4-dihydro-beta-carboline analogs of N-methyl-4-phenyl-1,2,3,6-tetrahydropyridine (MPTP) oxidation products. *Brain Res.* **1990**, *509* (1), 125−133.
(26) Bentley, M. C.; Almstetter, M.; Arndt, D.; Knorr, A.; Martin, E.; Pospisil, P.; Maeder, S. Comprehensive chemical characterization of the aerosol generated by a heated tobacco product by untargeted screening. *Anal. Bioanal. Chem.* **2020**, *412* (11), 2675−2685.
(27) Ho, B. T.; McIsaac, W. M.; Walker, K. E.; Estevez, V. Inhibitors of monoamine oxidase. Influence of methyl substitution on the inhibitory activity of $\beta$-carbolines. *J. Pharm. Sci.* **1968**, *57* (2), 269−274.
(28) Evans, G. J. The synaptosome as a model system for studying synaptic physiology. *Cold Spring Harb. Protoc.* **2015**, *2015* (5), 421−424.
(29) Benny, F.; Kumar, S.; Jayan, J.; Abdelgawad, M. A.; Ghoneim, M. M.; Kumar, A.; Manoharan, A.; Susan, R.; Sudevan, S. T.; Mathew, B. Review of $\beta$-carboline and its derivatives as selective MAO-A inhibitors. *Arch. Pharm.* **2023**, *356*, No. e2300091.
(30) Herraiz, T. Relative exposure to $\beta$-carbolines norharman and harman from foods and tobacco smoke. *Food Addit. Contam.* **2004**, *21* (11), 1041−1050.



https://doi.org/10.1021/acschemneuro.4c00789
ACS Chem. Neurosci. 2025, 16, 1117−1131

(31) Herraiz, T.; Chaparro, C. Human monoamine oxidase is inhibited by tobacco smoke: β-carboline alkaloids act as potent and reversible inhibitors. *Biochem. Biophys. Res. Commun.* **2005**, *326* (2), 378−386.
(32) Hogg, R. C. Contribution of Monoamine Oxidase Inhibition to Tobacco Dependence: A Review of the Evidence. *Nicotine Tob. Res.* **2016**, *18* (5), 509−523.
(33) Poindexter, E. H. J.; Carpenter, R. D. The isolation of harmane and norharmane from tobacco and cigarette smoke. *Phytochemistry* **1962**, *1* (1), 215−221.
(34) Rodgman, A.; Perfetti, T. A. *The Chemical Components of Tobacco and Tobacco Smoke*, 2nd ed.; CRC Press: Boca Raton, 2013; p 2332 doi.org/10.1201/b13973.
(35) Truman, P.; Atigari, D. V.; Kidwell, M.; Colussi-Mas, J.; Ellenbroek, B.The effect of mixed tobacco monoamine oxidase inhibitors in animal models relevant to tobacco dependence *Psychopharmacology* 2024 DOI: 10.1007/s00213-024-06712-8.
(36) Anderson, N. J.; Tyacke, R. J.; Husbands, S. M.; Nutt, D. J.; Hudson, A. L.; Robinson, E. S. In vitro and ex vivo distribution of [3H]harmane, an endogenous beta-carboline, in rat brain. *Neuropharmacology* **2006**, *50* (3), 269−276.
(37) Louis, E. D.; Rios, E.; Pellegrino, K. M.; Jiang, W.; Factor-Litvak, P.; Zheng, W. Higher blood harmane (1-methyl-9H-pyrido-[3,4-b]indole) concentrations correlate with lower olfactory scores in essential tremor. *Neurotoxicology* **2008**, *29* (3), 460−465.
(38) Guan, Y.; Louis, E. D.; Zheng, W. Toxicokinetics of tremorogenic natural products, harmane and harmine, in male Sprague-Dawley rats. *J. Toxicol. Environ. Health, Part A* **2001**, *64* (8), 645−660.
(39) Zetler, G.; Back, G.; Iven, H. Pharmacokinetics in the rat of the hallucinogenic alkaloids harmine and harmaline. *Naunyn-Schmiedeberg's Arch. Pharmacol.* **1974**, *285* (3), 273−292.
(40) Zetler, G.; Singbartl, G.; Schlosser, L. Cerebral pharmacokinetics of tremor-producing harmala and iboga alkaloids. *Pharmacology* **1972**, *7* (4), 237−248.
(41) Truman, P.; Grounds, P.; Brennan, K. A. Monoamine oxidase inhibitory activity in tobacco particulate matter: Are harman and norharman the only physiologically relevant inhibitors? *Neurotoxicology* **2017**, *59*, 22−26.
(42) Cho, H. U.; Kim, S.; Sim, J.; Yang, S.; An, H.; Nam, M. H.; Jang, D. P.; Lee, C. J. Redefining differential roles of MAO-A in dopamine degradation and MAO-B in tonic GABA synthesis. *Exp. Mol. Med.* **2021**, *53* (7), 1148−1158.
(43) Hovde, M. J.; Larson, G. H.; Vaughan, R. A.; Foster, J. D. Model systems for analysis of dopamine transporter function and regulation. *Neurochem. Int.* **2019**, *123*, 13−21.
(44) Wang, C.; Zhou, C.; Guo, T.; Huang, P.; Xu, X.; Zhang, M. Association between cigarette smoking and Parkinson's disease: a neuroimaging study. *Ther Adv. Neurol. Disord.* **2022**, *15*, No. 17562864221092566.
(45) Grella, B.; Dukat, M.; Young, R.; Teitler, M.; Herrick-Davis, K.; Gauthier, C. B.; Glennon, R. A. Investigation of hallucinogenic and related β-carbolines. *Drug Alcohol Depend.* **1998**, *50* (2), 99−107.
(46) Ferraz, C. A. A.; de Oliveira Junior, R. G.; Picot, L.; da Silva Almeida, J. R. G.; Nunes, X. P. Pre-clinical investigations of beta-carboline alkaloids as antidepressant agents: A systematic review. *Fitoterapia* **2019**, *137*, No. 104196.
(47) Glennon, R. A.; Dukat, M.; Grella, B.; Hong, S.; Costantino, L.; Teitler, M.; Smith, C.; Egan, C.; Davis, K.; Mattson, M. V. Binding of β-carbolines and related agents at serotonin (5-HT(2) and 5-HT(1A)), dopamine (D(2)) and benzodiazepine receptors. *Drug Alcohol Depend.* **2000**, *60* (2), 121−132.
(48) Edinoff, A. N.; Swinford, C. R.; Odisho, A. S.; Burroughs, C. R.; Stark, C. W.; Raslan, W. A.; Cornett, E. M.; Kaye, A. M.; Kaye, A. D. Clinically Relevant Drug Interactions with Monoamine Oxidase Inhibitors. *Health Psychol. Res.* **2022**, *10* (4), No. 39576.
(49) Ramakrishna, K.; Nalla, L. V.; Naresh, D.; Venkateswarlu, K.; Viswanadh, M. K.; Nalluri, B. N.; Chakravarthy, G.; Duguluri, S.; Singh, P.; Rai, S. N.; et al. WNT-β Catenin Signaling as a Potential Therapeutic Target for Neurodegenerative Diseases: Current Status and Future Perspective. *Diseases* **2023**, *11* (3), No. 89.
(50) Kumar, S.; Nair, A. S.; Bhashkar, V.; Sudevan, S. T.; Koyiparambath, V. P.; Khames, A.; Abdelgawad, M. A.; Mathew, B. Navigating into the Chemical Space of Monoamine Oxidase Inhibitors by Artificial Intelligence and Cheminformatics Approach. *ACS Omega* **2021**, *6* (36), 23399−23411.
(51) The Binding Database. https://www.bindingdb.org/rwd/bind/index.jsp.
(52) Chen, X.; Lin, Y.; Gilson, M. K. The binding database: overview and user's guide. *Biopolymers* **2001**, *61* (2), 127−141.
(53) Chen, X.; Liu, M.; Gilson, M. K. BindingDB: a web-accessible molecular recognition database. *Comb. Chem. High Throughput Screening* **2001**, *4* (8), 719−725.
(54) von Korff, M.; Freyss, J.; Sander, T. Flexophore, a new versatile 3D pharmacophore descriptor that considers molecular flexibility. *J. Chem. Inf Model* **2008**, *48* (4), 797−810.
(55) Sander, T.; Freyss, J.; von Korff, M.; Rufener, C. DataWarrior: an open-source program for chemistry aware data visualization and analysis. *J. Chem. Inf. Model.* **2015**, *55* (2), 460−473.
(56) Crystal Structure of Human Monoamine Oxidase A with Harmine. https://www.rcsb.org/structure/2z5x (accessed July 20, 2007).
(57) Son, S. Y.; Ma, J.; Kondou, Y.; Yoshimura, M.; Yamashita, E.; Tsukihara, T. Structure of human monoamine oxidase A at 2.2-A resolution: the control of opening the entry for substrates/inhibitors. *Proc. Natl. Acad. Sci. U.S.A.* **2008**, *105* (15), 5739−5744.
(58) Structure of human MAO B in complex with the selective inhibitor safinamide. https://www.rcsb.org/structure/2V5Z (accessed July 12, 2007).
(59) Binda, C.; Wang, J.; Pisani, L.; Caccia, C.; Carotti, A.; Salvati, P.; Edmondson, D. E.; Mattevi, A. Structures of human monoamine oxidase B complexes with selective noncovalent inhibitors: safinamide and coumarin analogs. *J. Med. Chem.* **2007**, *50* (23), 5848−5852.
(60) Berman, H. M.; Westbrook, J.; Feng, Z.; Gilliland, G.; Bhat, T. N.; Weissig, H.; Shindyalov, I. N.; Bourne, P. E. The Protein Data Bank. *Nucleic Acids Res.* **2000**, *28* (1), 235−242.
(61) Chemical Computing Group (CCG). Computer-Aided Molecular Design (chemcomp.com). Chemical Computing Group ULC. https://www.chemcomp.com/index.htm.
(62) Corbeil, C. R.; Williams, C. I.; Labute, P. Variability in docking success rates due to dataset preparation. *J. Comput. Aided Mol. Des.* **2012**, *26* (6), 775−786.
(63) Shen, J.; Cheng, F.; Xu, Y.; Li, W.; Tang, Y. Estimation of ADME properties with substructure pattern recognition. *J. Chem. Inf. Model.* **2010**, *50* (6), 1034−1041.
(64) Egan, W. J.; Merz, K. M., Jr.; Baldwin, J. J. Prediction of drug absorption using multivariate statistics. *J. Med. Chem.* **2000**, *43* (21), 3867−3877.
(65) van der Toorn, M.; Koshibu, K.; Schlage, W. K.; Majeed, S.; Pospisil, P.; Hoeng, J.; Peitsch, M. C. Comparison of monoamine oxidase inhibition by cigarettes and modified risk tobacco products. *Toxicol. Rep.* **2019**, *6*, 1206−1215.
(66) Jørgensen, S.; Nielsen, E. O.; Peters, D.; Dyhring, T. Validation of a fluorescence-based high-throughput assay for the measurement of neurotransmitter transporter uptake activity. *J. Neurosci. Methods* **2008**, *169* (1), 168−176.
(67) Bernstein, A. I.; Stout, K. A.; Miller, G. W. A fluorescent-based assay for live cell, spatially resolved assessment of vesicular monoamine transporter 2-mediated neurotransmitter transport. *J. Neurosci. Methods* **2012**, *209*, 357−366, DOI: 10.1016/j.jneumeth.2012.06.002.